# Overcoming the Genotoxicity of a Pyrrolidine Substituted Arylindenopyrimidine As a Potent Dual Adenosine A(2A)/A(1) Antagonist by Minimizing Bioactivation to an Iminium Ion Reactiv...

**ARTICLE** *in* CHEMICAL RESEARCH IN TOXICOLOGY · JUNE 2011

Impact Factor: 3.53 · DOI: 10.1021/tx1004437 · Source: PubMed

Chemical Research in Toxicology

ARTICLE

pubs.acs.org/crt

# Overcoming the Genotoxicity of a Pyrrolidine Substituted Arylindenopyrimidine As a Potent Dual Adenosine $A_{2A}/A_1$ Antagonist by Minimizing Bioactivation to an Iminium Ion Reactive Intermediate

Heng-Keang Lim,*[,†] Jie Chen,[†] Carlo Sensenhauser,[†] Kevin Cook,[†] Robert Preston,[†] Tynisha Thomas,[†] Brian Shook,[‡] Paul F. Jackson,[‡] Stefanie Rassnick,[§] Kenneth Rhodes,[§] Vedwatee Gopaul,[†] Rhys Salter,[†] Jose Silva,[†] and David C. Evans[†]

[†]Drug Safety Sciences, [‡]Medicinal Chemistry, and [§]Biology, Johnson and Johnson Pharmaceutical Research and Development, 1000 Route 202 South, New Jersey 08869, United States

Supporting Information

**ABSTRACT:**

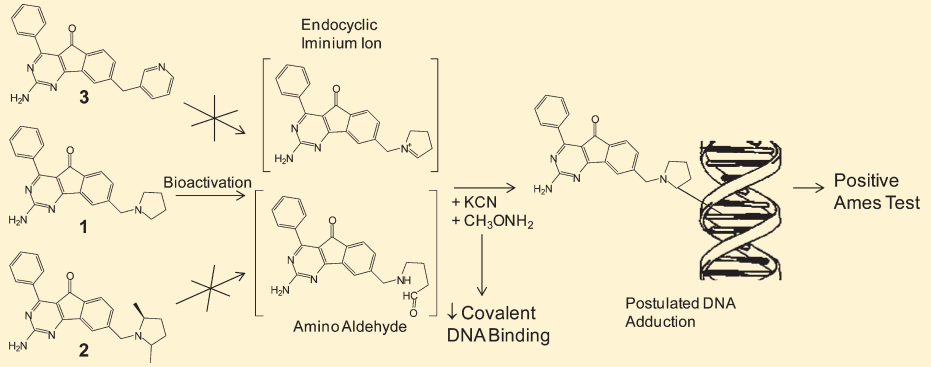


2-Amino-4-phenyl-8-pyrrolidin-1-ylmethyl-indeno[1,2-d]pyrimidin-5-one (**1**) is a novel and potent selective dual $A_{2A}/A_1$ adenosine receptor antagonist from the arylindenopyrimidine series that was determined to be genotoxic in both the Ames and Mouse Lymphoma L5178Y assays only following metabolic activation. Compound **1** was identified as a frame-shift mutagen in *Salmonella typhimurium* tester strain TA1537 as indicated by a significant dose-dependent increase in revertant colonies as compared to the vehicle control. The metabolic activation-dependent irreversible covalent binding of radioactivity to DNA, recovery of **1** and its enamine metabolite from acid hydrolysis of covalently modified DNA, and protection of covalent binding to DNA by both cyanide ion and methoxylamine suggest that the frame-shift mutation in TA1537 strain involved covalent binding instead of simple intercalation to DNA. Compound **1** was bioactivated to endocyclic iminium ion, aldehyde, epoxide, and $\alpha,\beta$-unsaturated keto reactive intermediates from the detection of cyano, oxime, and glutathione conjugates by data-dependent high resolution accurate mass measurements. Collision-induced dissociation of these conjugates provided evidence for bioactivation of the pyrrolidine ring of **1**. The epoxide and $\alpha,\beta$-unsaturated keto reactive intermediates were unlikely to cause the genotoxicity of **1** because the formation of their glutathione adducts did not ameliorate the binding of compound related material to DNA. Instead, the endocyclic iminium ions and amino aldehydes were likely candidates responsible for genotoxicity based on, first, the protection afforded by both cyanide ion and methoxylamine, which reduced the potential to form covalent adducts with DNA, and, second, analogues of **1** designed with low probability to form these reactive intermediates were not genotoxic. It was concluded that **1** also had the potential to be mutagenic in humans based on observing the endocyclic iminium ion following incubation with a human liver S9 preparation and the commensurate detection of DNA adducts. An understanding of this genotoxicity mechanism supported an evidence-based approach to selectively modify the structure of **1** which resulted in analogues being synthesized that were devoid of a genotoxic liability. In addition, potency and selectivity against both adenosine $A_{2A}$ and $A_1$ receptors were maintained.

## INTRODUCTION

Parkinson's disease (PD) is characterized by a progressive impairment of motor function, which is due to the gradual degeneration of dopaminergic neurons in the pars compacta region of the substantia nigra and their projections through the nigrostriatal pathway to the caudal putamen.[1] The majority of medical therapies for PD are aimed at restoring dopamine (DA) signaling using L-dihydroxyphenylalanine (DOPA) as monotherapy or in combination with a peripheral DOPA-decarboxylase

**Received:** December 19, 2010
**Published:** June 13, 2011

inhibitor or with an inhibitor of DA turnover by inhibition of monoamine oxidase B or catechol *O*-methyltransferase.[1] These DA targeted therapies are all effective in treating motor dysfunction but produce undesirable side effects. Moreover, they lose efficacy with treatment since they neither alter disease progression nor treat comorbidities from progressive degeneration of nondopaminergic brain systems. As a result, drug companies seek more effective nondopaminergic based treatments for PD without these liabilities. One such nondopaminergic approach is by antagonism of $A_{2A}$ and $A_1$ receptors, which provides synergistic improvement in DA signaling by enhancing postsynaptic responses to DA and DA release, respectively.

Lead optimization of an arylindenopyrimidine series of compounds resulted in analogues substituted at the 8- and 9-positions with greater *in vitro* functional antagonism of $A_{2A}$ over $A_1$ receptors.[2] However, 8-substituted analogues consistently gave greater *in vivo* potency when tested in the haloperidol-induced catalepsy mouse model. This led to the discovery of 2-amino-4-phenyl-8-pyrrolidin-1-ylmethyl-indeno[1,2-d]pyrimidin-5-one (**1**, Figure 1). Compound **1** is a novel, selective and potent dual $A_{2A}/A_1$ adenosine receptor antagonist as indicated by $K_i$ values (mean ± SE of 3 experiments) of 17.0 ± 4.4, 4.1 ± 0.9, 97.0 ± 6.1, and 22.8 ± 7.3 nM from *in vitro* functional evaluation of **1** for the antagonism of adenosine $A_1$, $A_{2A}$, $A_{2B}$, and $A_3$ receptor subtypes, respectively. Furthermore, **1** displayed dose-dependent efficacy in several pharmacological models for evaluating PD such as the reversal of neuroleptic-induced catalepsy in both mice and rats, reversal of reserpine-induced akinesia in mice, and increased contralateral rotations in 6-hydroxydopamine-lesioned rats by DOPA. A minimum effective oral dose of 1 mg/kg was obtained in each animal model for evaluating PD, which suggests that **1** possesses potential anti-Parkinsonian properties. In addition, it had good systemic exposure after oral dosing due to acceptable ADME properties, and did not have any safety pharmacology and toxicology adverse findings. Overall, **1** had the potential to be a drug development candidate.

However, **1** registered a positive finding only in the *Salmonella typhimurium* strain TA1537 in the presence of NADPH-fortified Aroclor 1254-induced rat S9 when evaluating in the GLP 5-strain Ames assay. Further genotoxicity testing in the Mouse Lymphoma L5178Y assay again indicated that **1** was only mutagenic with metabolic activation. Data from both genotoxicity studies implied that a metabolite instead of **1** was responsible for its mutagenicity. As a result, **1** was not progressed further in preclinical development. However, there was an urgent need to elucidate the mechanism of mutagenicity of **1** in order to address the viability of the arylindenopyrimidine scaffold and to provide direction to the backup chemistry program to design an analogue without this liability.

We investigated the mechanism of mutagenicity of **1** in the Ames test by assessing covalent binding to DNA following the incubation of **1** in Aroclor 1254-induced rat liver S9 in the presence and absence of NADPH. We also investigated the ability of chemical nucleophiles to protect DNA from being labeled by drug related material. The structures of the reactive intermediates from the *in vitro* metabolism of **1** were elucidated from trapping experiments with nucleophiles. The relevance of the preclinical mutagenicity findings of **1** to humans was investigated using NADPH-fortified human liver S9. An understanding of the bioactivation mechanism leading to genotoxicity led to the synthesis of specific analogues of **1**, which provided products that were not genotoxic.

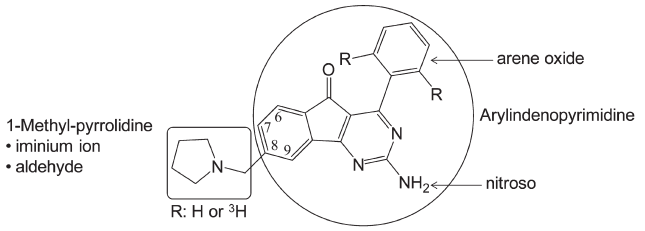


**1**: 2-amino-4-phenyl-8-pyrrolidin-1-ylmethyl-indeno[1,2-d]pyrimidin-5-one (MW: 356)

$A_{2A}$ $K_i$: 4.1 nM, $A_1$ $K_i$: 17.0 nM, $ED_{50}$, po: 0.2 mg/kg

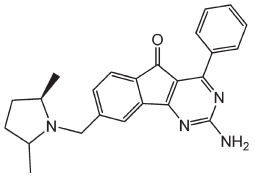

**2**: 2-amino-8-(2,5-dimethyl-pyrrolidin-1-ylmethyl)-4-phenyl-indeno[1,2-d]pyrimidin-5-one (MW: 384)

$A_{2A}$ $K_i$: 13.1 nM, $A_1$ $K_i$: 37.3 nM, $ED_{50}$, po: 3.2 mg/kg

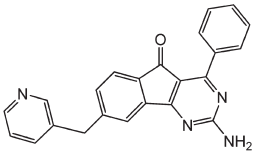

**3**: 2-amino-4-phenyl-8-pyridin-3-ylmethyl-indeno[1,2-d]pyrimidin-5-one (MW: 364)

$A_{2A}$ $K_i$: 0.5 nM, $A_1$ $K_i$: 3.5 nM, $ED_{50}$, po: <1.0 mg/kg

**Figure 1.** Chemical structures and pharmacological activities of compounds **1**, **2**, and **3** used for the evaluation of genotoxicity potential in the GLP 5-strain reversal mutation Ames test. Potential structural alerts for the formation of postulated reactive intermediates were displayed for **1**.

## EXPERIMENTAL PROCEDURES

**Chemicals.** Ethylenediaminetetraacetic acid (EDTA) disodium salt, 0.5 M, 1.0 M magnesium chloride ($MgCl_2$), 1.0 M phosphate buffer, pH 7.4, calf thymus DNA (Type XV), ammonium acetate (Sigma Ultra grade), glutathione (GSH), potassium cyanide (KCN), trifluoroacetic acid (TFA), methoxylamine, nefazodone, benzyl-2-pyrrolidinone, benzyl-3-pyrrolidinone, pyridine, $D_2O$ (99.9% D), acetonitrile-$d_3$ (99.96% D), formic acid-$d_2$ (98% D), reduced nicotinamide adenine dinucleotide phosphate (NADPH), DNase I, phosphodiesterase I, and alkaline phosphatase were purchased from Sigma-Aldrich (St. Louis, MO). NADPH-regenerating system solutions A and B and pooled mixed gender human liver S9 were obtained from BD BioSciences (Woburn, MA). [$^{14}$C]-Benzo[*a*]pyrene and [$^3$H]-**1** were obtained from Movarek Biochemicals, Inc. (Brea, CA). [$^{13}C_2$ $^{15}$N-Gly]GSH, K$^{13}$C$^{15}$N and methoxyl-$d_3$-amine were from Cambridge Isotope Laboratories, Inc. (Andover, MA). HPLC grade water and acetonitrile were bought from EMD Chemicals, Inc. (Gibbstown, NJ). Aroclor 1254-induced Sprague−Dawley rat liver S9 were from MOLTOX (Boone, NC). *Salmonella typhimurium* strains TA98, TA100, TA1535, and TA1537 were obtained from Dr. B. Ames (Berkeley, CA), and *Escherichia coli* strain $WP_2$uvrA was obtained from Dr. S. Haworth (Bethesda, MD). The arylindenopyrimidinyl analogues used were from Johnson and Johnson Pharmaceutical Research and Development (Spring House, PA). γ-Lactam-**1**, enamine-**1**, and 2,5-dicyanopyrrolidinyl-**1** were isolated from *in vitro* incubations.

**Ames Test.** The Ames test was conducted using *S. typhimurium* strains TA98, TA100, TA1535, and TA1537 and *Escherichia coli* strain $WP_2$uvrA by an adaptation of the procedure from the published Ames test[3] and that briefly described here. Two milliliters of molten top agar

containing 0.1 mL of bacteria strain in broth and 0.5 mL of either phosphate buffer or Aroclor 1254-induced rat liver S9 with a NADPH regenerating system were added to tubes containing the test compound. Initial testing of the compound was conducted at single concentrations of 0, 5, 10, 25, 50, 100, 250, 500, 1000, 2500, and 5000 $\mu$g/plate except in triplicate for the vehicle control. The compound testing positive was retested under GLP conditions at concentrations ($n$ = 6) of 0, 10, 50, 100, 250, 333, 500, 750, and 1000 $\mu$g/plate. A negative vehicle control (DMSO) and 5 positive controls (dexon {*p*-dimethylaminobenzenediazo sulfonate} [TA98], 9-aminoacridine HCl [TA1537], sodium azide [TA100 and TA1535], 4-nitroquinolone [$WP_2$uvrA], and 2-anthramine [all strains]) were also included in the same analysis, and each test condition was conducted in triplicate. A complete study was composed of duplicate independent experiments. The contents of each tube were vortexed and quickly poured onto labeled Petri dishes containing 25 ± 2 mL bottom agar and gently swirled to ensure even layering of the top agar. The dishes were allowed to cool at room temperature and then transferred to an incubator where they remained for 48 to 72 h at 37 °C. Visible revertant bacterial colonies were counted and recorded, and the mean ± SEM were calculated. A test compound is considered positive if it induced a dose-dependent 2-fold (TA98, TA100, and $WP_2$uvrA) and 3-fold (TA1535 and TA1537) increase in the number of revertant colonies over the negative vehicle-treated controls.

***In Vitro* Covalent Binding of [$^3$H]-1 to DNA.** The potential for covalent binding of **1** to DNA was evaluated *in vitro* in the absence and presence of metabolic activation to simulate conditions encountered in the Ames test by modification of a previously reported procedure.[4] All incubations, final volume of 1 mL, consisted of 1 mg/mL calf thymus DNA, 2 mg/mL Aroclor 1254-induced rat liver S9, 4 mM $MgCl_2$, 2 mM EDTA, 100 $\mu$M **1** (97.3 $\mu$M **1** + 2.7 $\mu$M [$^3$H]-**1**; specific activity, 3.7 Ci/mmol; concentration, 1mCi/mL), or [$^{14}$C]-benzo[*a*]pyrene (100 $\mu$M, positive control; specific activity, 26.6 mCi/mmol, 100 $\mu$Ci/mL), 2.5 mM NADPH, and 0.1 M phosphate buffer at pH 7.4. The Aroclor 1254-induced rat liver S9 was replaced by human liver S9 to assess the human relevance of the genotoxicity of **1**. [$^{14}$C]-Benzo[*a*]pyrene and [$^3$H]-**1** were dissolved in ethanol and DMSO, respectively, and the amount of organic solvent in the final incubation was 1% (v/v). Appropriate control incubations were also included such as incubations containing only the solvent vehicle, the absence of S9, boiled human liver S9, or the absence of NADPH. The protective effect of chemical nucleophiles on the covalent binding of **1** to DNA was investigated in the presence of 2 mM KCN, 2 mM methoxylamine, or 5 mM GSH. The mixtures were incubated in duplicate or triplicate at 37 °C for 2 h prior to the termination of the reaction by the removal of unbound test compound and its metabolites via liquid−liquid extraction using 5 mL of phenol/chloroform/isoamyl alcohol (25:24:1). After centrifugation at 1,203*g* for 10 min at 5 °C, the upper layer containing the DNA was transferred to another tube for 2 additional extractions with 2 mL of chloroform/isoamyl alcohol (24:1) prior to centrifugation as before. The bottom layer containing the proteins was discarded. The DNA was precipitated by the addition of 10 mL of 2 M NaCl and 2 mL of ethanol, and the resultant pellet from the above centrifugation was extracted twice with 2 mL of ethanol or until radioactivity approached background levels before dissolving in 1 mL of Tris-EDTA for the determination of DNA concentration by UV spectroscopy at 260 nm and covalent binding to DNA by liquid scintillation counting in a Packard TriCarb 3100TR LSC (Perkin-Elmer LAS, Shelton, CT). The data was expressed as the mean of pmol of covalently bound radioactivity per mg DNA.

Alternatively, the covalently modified DNA was solubilized in 0.5 mL of 10 mM Tris HCl/$MgCl_2$ buffer 7.0, and an aliquot of 230 $\mu$L was used for enzymatic hydrolysis[5] with 1300 units DNase I, 0.06 units phosphodiesterase I, and 380 units of alkaline phosphatase at 37 °C for 2 h. Acid hydrolysis[6] was carried out by adding an aliquot of 20 $\mu$L of concentrated formic acid to 230 $\mu$L of DNA solution from above prior to heating at 80 °C for 1 h. The enzyme- or acid-hydrolyzed sample was treated with 6 volumes of acetonitrile and vortexed prior to centrifugation at 1,203*g* for 10 min at 5 °C. The supernatant was transferred to a clean tube and dried at room temperature under a gentle stream of nitrogen. The residue was reconstituted in 250 $\mu$L of water/acetonitrile (9:1) containing 0.01% formic acid, sonicated, and hand-vortexed to dissolve the residue. The solution was then filtered by centrifugation through a 0.45 $\mu$m nylon filter at 7,200*g* for 10 min at room temperature. Both filtered enzyme- and acid-hydrolyzed samples were analyzed by liquid chromatography−radioactivity detector−mass spectrometry (LC-RAD-MS).

**Reactive Intermediate Trapping Studies.** The trapping experiments were conducted by the modification of a previously reported procedure.[7] All incubations, 1 mL final volume, consisted of 2 mM EDTA, 5 mM $MgCl_2$, 2 mg/mL S9, 100 $\mu$M test compound or nefazodone (positive control), 5 mM of a 2:1 ratio of GSH:[$^{13}C_2$$^{15}$N-Gly]GSH, 2 mM of a 2:1 ratio of KCN:K$^{13}$C$^{15}$N, or 2 mM of a 2:1 ratio of methoxylamine:methoxyl-$d_3$-amine, 3.3 mM glucose-6-phosphate, 0.4 units/mL glucose-6-phosphate dehydrogenase, 1.3 mM $NADP^+$, and 0.1 M phosphate buffer, pH 7.4. Incubations without either NADPH regenerating system or trapping agents were included as negative controls. Typically, reagents were prepared in 0.1 M phosphate buffer (pH 7.4), except for the drug, which was spiked as 10 $\mu$L of 5 mM in acetonitrile/$H_2O$ (1:1) stock solution to keep the final acetonitrile content <1%. After incubation for 1 h at 37 °C in an open tube, the incubation was terminated by the addition of 6 mL of acetonitrile, and the tube was vortexed prior to centrifugation at 1,203*g* for 10 min at 5 °C. The supernatant was transferred to a clean tube and dried at room temperature under a gentle stream of nitrogen. The residue was reconstituted in 250 $\mu$L of water/acetonitrile (9:1) containing 0.01% formic acid, sonicated, and hand-vortexed to dissolve the residue. The solution was then filtered by centrifugation through a 0.45 $\mu$m nylon filter at 7,200*g* for 10 min at room temperature. The filtrate was transferred to a 96-well plate for analysis by liquid chromatography−mass spectrometry (LC-MS).

**Quantification of Iminium Ions.** The incubation of **1** for the quantification of iminium ions was modified from previous conditions used for trapping reactive intermediates. All incubations, 1-mL total volume, consisted of 2 mM EDTA, 4 mM $MgCl_2$, 2 mg/mL S9, 100 $\mu$M **1**, 2 mM of a 2:1 ratio of KCN (1.35 mM):K$^{13}$C$^{15}$N (0.3 mM)+K$^{14}$CN (0.35 mM; specific activity, 56.0 mCi/mmol; concentration, 1 mCi/mL), 1.5 mM NADPH, and 0.1 M phosphate buffer, pH 7.4. The samples were processed as described previously for trapping reactive intermediates except for final reconstitution in 500 $\mu$L prior to loading onto Strata X SPE cartridges (30 mg/mL; Phenomenex, Torrance, CA), which have been conditioned as suggested by the vendor. The Strata X SPE cartridges were sequentially washed with 1 mL each of 5 and 10% (v/v) methanol in water prior to elution with 1 mL of methanol. The methanol fractions were dried at room temperature under a gentle stream of nitrogen. The residue in each tube was handled as described previously for trapping reactive intermediates prior to analysis by LC-RAD-MS.

**LC-MS Analysis.** All screening of cyano, oxime, and glutathione conjugates were carried out using an Agilent 1100 LC system (Agilent, Santa Clara, CA) coupled to a LTQ (Thermo Scientific, Inc., San Jose, CA) or an Accela LC system (Thermo Scientific, Inc., San Jose, CA) coupled to a LTQ/Orbitrap (Thermo Scientific, Inc., Bremen, Germany). Analysis by either mass spectrometer was conducted in the positive electrospray ionization (ESI) mode. An aliquot (20 to 50 $\mu$L) of reconstituted sample was injected for chromatographic separation on a HyPurity Aquastar column (100 or 150 × 2.1 mm ID, 3 $\mu$m [Thermo Fisher Scientific, Inc., Bellefonte, PA]) thermoregulated at 50 °C. The chromatographic separation was by gradient elution started at 5% B for 0.5 min, increased nonlinearly to 95% B over 17 min (with the rate of increase ranging from 2 to 8.8% B/min), held at 95% B over 2 min, and

then returned to 5% B over 1 min. An alternate method with greater chromatographic resolution was achieved using a 150 × 2.1 mm ID Kinetex C18 column packed with 2.6 μm and 100 Å particles (Phenomenex, Torrance, CA). The LC gradient started at 3% B for 2 min, increased nonlinearly to 95% B over 28 min (with the rate of increase ranging from 0.5 to 5% B/min), held at 95% B over 5 min, and then returned to 3% B over 1 min. Solvents A and B corresponded to water and acetonitrile containing 0.2% (v/v) formic acid. The flow rate was set at 400 μL/min and split postcolumn 1:1 with half the eluant sprayed into the mass spectrometer at +5 kV with nebulizer, sheath, and sweep gases set at 65, 20, and 5 arbitrary units, respectively. The desolvation of the solvent droplets was further aided by a heated capillary temperature of 300 °C. The mass spectrometer was optimized by the infusion of 5 ng/μL of **1** in 50:50 acetonitrile/water directly into 50:50 mobile phases A and B at 0.2 mL/min. The cyano, oxime, and glutathione conjugates were screened by isotopic pattern triggered data-dependent multiple-stage nominal mass analysis by modification of the MS method described elsewhere.[7] The cyano, oxime, or glutathione conjugates were initially detected by full scan nominal mass analysis from *m/z* 150 to 1000, and only conjugates with the desired isotopic pattern (cyano conjugates, 2 Da mass delta and ratio of 0.5; oxime and glutathione conjugates, 3 Da mass delta and ratio of 0.4) automatically triggered $MS^2$, $MS^3$, and $MS^4$ analyses. The tolerance of the isotopic ratio was set to ±0.1 of the set value. Collision-induced dissociation (CID) was conducted using an isolation width of 2 Da, activation *q* of 0.25, an activation time of 30 ms, and normalized collision energies of 20%, 20%, and 30% for $MS^2$, $MS^3$, and $MS^4$, respectively. Collision energy was adjusted as needed to ensure more than 80% attenuation of the precursor ion. Ions were detected with electron multipliers 1 and 2 set at 795 and 815 V, respectively. Data acquisition and reduction were carried out using Xcalibur 2.0 (San Jose, CA).

Confirmation of the detected conjugates using the LTQ/Orbitrap (Thermo Scientific, Inc., Bremen, Germany) was as previously reported[7] except that mass measurement was carried out under internal mass calibration mode unless otherwise indicated. The internal mass calibrant, tamoxifen at 10 pg/uL in 95:5 acetonitrile/water containing 0.01% formic acid, was introduced as the sheath flow at 75 μL/min directly into the ESI source. The stability of the intensity of the internal mass calibrant was verified prior to analysis. The cyano, oxime, and glutathione conjugates were detected by full scan accurate mass analysis from *m/z* 150 to 1000 at a resolving power of 60,000 at *m/z* 400 fwhm (full width at half-maximum). The isotopic patterns used to trigger data-dependent scans were as described for the nominal mass above. CID was conducted with normalized collision energies of 28% ($MS^2$) and 45% ($MS^3$) for cyano conjugates, while an equal normalized collision energy of 30% was used for both $MS^2$ and $MS^3$ analyses of oxime conjugates. Lower normalized collision energies of 22% ($MS^2$), 25% ($MS^3$), 28% ($MS^4$), and 35% ($MS^4$) were used for GSH conjugates. The rest of the conditions used were the same as those reported.[7]

The full scan MS and $MS^2$ nominal and accurate mass data were processed using MetWorks 1.1.0 and Qual Browser (Thermo Scientific, Inc., Bremen, Germany), respectively. The full scan nominal MS data was interrogated for cyano conjugates by filtering for isotopic pattern with a mass delta of 2 and isotope ratios of 0.5 (+1 cyano) and 0.97 (+2 cyano). The detection of both oxime and glutathione conjugates was also by filtering of full scan nominal mass data for isotopic pattern with a mass delta of 3 and an isotopic ratio of 0.4. In addition, the $MS^2$ data from data-dependent scans was processed for cyano and glutathione conjugates using a neutral mass loss of 27 and 129 Da, respectively. Furthermore, the accurate MS and $MS^2$ data were processed for both cyano and glutathione conjugates using procedures which have been described elsewhere.[7]

**LC-RAD-MS Analysis.** All analyses of reconstituted radiolabeled samples were analyzed using a Surveyor Plus or Accela LC system (Thermo Scientific, Inc., San Jose, CA) coupled to an accurate radioisotope counting, dynamic-flow radioactivity detector (RAD, AIM Research Company, Hockessin, DE) and a LXQ or LTQ (Thermo Scientific, Inc., San Jose, CA) operated in the positive ESI mode. The LC eluant was split postcolumn 1:1 to both RAD and MS for simultaneous quantification by RAD and detection by MS. The RAD was operated by an adaptation of procedures reported elsewhere.[8] All radiolabeled samples were analyzed using a 150 × 2.1 mm ID Synergi Fusion-RP column packed with 4 μm and 80 Å particles (Phenomenex, Torrance, CA). The chromatographic separation of reconstituted enzyme- and acid-hydrolyzed DNA samples were carried out using an LC gradient, which was held at 95% A (10 mM ammonium acetate containing 0.02% TFA):5% B (10 mM ammonium acetate in methanol containing 0.02% TFA) for 5 min and eluted at 400 μL/min with a linear gradient from 5 to 95% B over 30 min. All other conditions were as described in the Experimental Procedures section on LC-MS analysis.

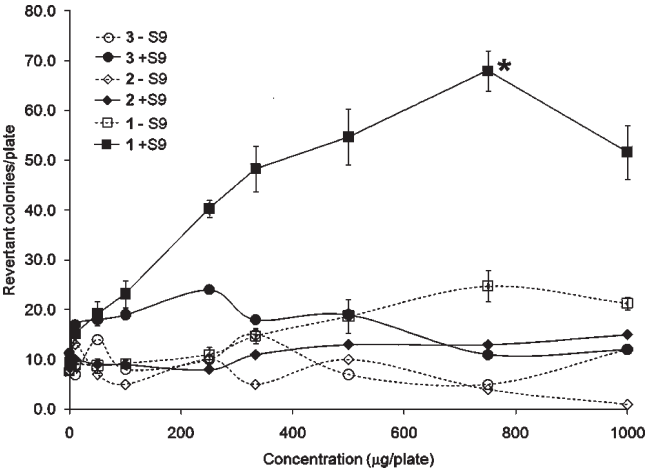


**Figure 2.** Compounds **1**, **2**, and **3** were evaluated for genotoxicity in the reverse mutation Ames test in 5 bacterial strains, but we only present data from the *Salmonella typhimurium* strain TA1537. The genotoxicity of each compound was evaluated in the presence and absence of Aroclor 1254-induced rat liver S9. The data of compound **1** was from the average of 6 plates ± SEM compared to the single plate for compounds **2** and **3**. Data points with asterisks corresponded to those at least 3-fold greater than the vehicle control and statistically significant by *t*-test at $p \leq 0.05$.

All quantification of cyano conjugates was carried out using the LC-RAD-MS system above except for the LC gradient used for the chromatographic separation of conjugates. The LC gradient was held at 90% A (2.5 mM ammonium acetate)/10% B (acetonitrile) for 0.5 min and eluted at 400 μL/min with a nonlinear gradient from 10 to 95% B over 22.5 min (rate of increase of 5.2% B/min over first 9.5 min, decreased to 1.8% B/min over 12 min, and finally increased to 15% B/min), held at 95% B over 2 min, and then returned to 10% B over 5 min. Other conditions were as described in the Experimental Procedures section on LC-MS analysis.

**Microderivatization and Online Hydrogen/Deuterium (H/D) Exchange.** Derivatization of the keto group was by heating an equal volume of a methanolic solution of an *in vitro* incubate of **1** and pyridine or spiked with an equal volume of 20 μM benzyl-3-pyrrolidinone or benzyl-2-pyrrolidinone and 0.2 M of methoxylamine dissolved in pyridine at 80 °C for 1 h.[9] The excess methoxylamine was removed by adding 1 mL of 1 N HCl and vortexed for 5 min. The solution was then neutralized with 1 N KOH, adjusted to pH 11 with concentrated ammonium hydroxide (~100 μL) and saturated with NaCl prior to liquid−liquid extraction with 6 mL of ethyl acetate for 15 min. The tubes were centrifuged at 1,203*g* for 10 min at 5 °C, and the supernatant was transferred to clean glass tubes prior to evaporation to dryness as

**Table 1.**[a]

| incubation | covalent DNA binding (pmol/mg) |
|---|---|
| | mean ± SD |
| vehicle (DMSO) + DNA | 3.8 ± 1.0 |
| [$^{14}$C]-benzo[*a*]pyrene (100 $\mu$M) + DNA | 47.3 ± 8.1 |
| [$^{14}$C]-benzo[*a*]pyrene (100 $\mu$M) + DNA + Aroclor 1254-induced rat liver S9 | 110.7 ± 5.7 |
| [$^{14}$C]-benzo[*a*]pyrene (100 $\mu$M) + DNA + Aroclor 1254-induced rat liver S9 + NADPH | 1341.0 ± 84.5 |
| vehicle (ethanol) + DNA | 0.7 ± 0.2 |
| [$^{3}$H]-**1** (100 $\mu$M) +DNA | 13.7 ± 1.7 |
| [$^{3}$H]-1 (100 $\mu$M + DNA + Aroclor 1254-induced rat liver S9 | 17.5 ± 0.8 |
| [$^{3}$H]-1 (100 $\mu$M) + DNA + Aroclor 1254-induced rat liver S9 + NADPH | 247.8 ± 12.7 |
| [$^{3}$H]-**1** (100 $\mu$M) + DNA + boiled human liver S9 | 16.9 (15.6, 18.1) |
| [$^{3}$H]-1 (100 $\mu$M) + DNA + human liver S9 | 46.3 (45.2, 47.4) |
| [$^{3}$H]-1 (100 $\mu$M) + DNA + human liver S9 + NADPH | 83.7 (83.8, 83.5) |
| [$^{3}$H]-1 (100 $\mu$M) + DNA + Aroclor 1254-induced rat liver S9 + NADPH | 100% (194.5:193.2,195.7) |
| [$^{3}$H]-1 (100 $\mu$M) + DNA + Aroclor 1254-induced rat liver S9 + KCN + NADPH | 42.3% (82.3: 78.8, 86.1) |
| [$^{3}$H]-1 (100, $\mu$M) + DNA + Aroclor 1254-induced rat liver S9 + methoxylamine + NADPH | 54.3% (105.7: 105.6, 105.8) |
| [$^{3}$H]-1 (100, $\mu$M) + DNA + Aroclor 1254-induced rat liver S9 + KCN + methoxylamine + NADPH | 5.3 ± 0.8 |
| [$^{3}$H]-1 (100 $\mu$M) + DNA + Aroclor 1254-induced rat liver S9 + glutathione + NADPH | 97.3% (189.4: 190.4, 188.4) |

[a] Assessment of covalent binding to DNA was from the incubation of 1 mg/mL calf thymus DNA with the vehicle (DMSO or ethanol), [$^{14}$C]-benzo[*a*]pyrene (100 $\mu$M, positive control), or [$^{3}$H]-**1**:**1** (2.7:97.3 $\mu$M) for 2 h at 37 °C. Similar incubations were also carried out with [$^{14}$C]-benzo[*a*]pyrene or [$^{3}$H]-**1**:**1** in Aroclor 1254-induced rat liver S9 with and without NADPH. Covalent binding to DNA was also investigated using human liver S9. The effect of KCN, methoxylamine, or glutathione on the covalent binding of [$^{3}$H]-**1**:**1** to DNA was investigated in Aroclor 1254-induced rat liver S9 supplemented with NADPH. Isolated DNA pellet was extracted with ethanol prior to resuspension for the quantification of DNA-bound compound by scintillation counting and DNA quantification by UV spectroscopy at 260 nm. Covalent binding to DNA was expressed as the mean ± SD in pmol/mg DNA for triplicate and mean (range) for duplicate analyses.

described previously. The residue from either derivatization procedure was processed as described for trapping reactive intermediates prior to LC-MS analysis. The online H/D exchange was conducted using the LC-MS conditions with greater chromatographic resolution but with replacement of the solvent system with $D_2O$ and acetonitrile-$d_3$ containing 0.2% (v/v) of formic acid-$d_2$. The efficiency of H/D exchange was evaluated with **1** prior to the analysis of samples.

## RESULTS

**Genotoxicity Testing.** The assessment of mutagenicity in a bacterial reverse mutation (Ames) test is one of the recommended test batteries for the evaluation of genotoxicity by regulatory agencies for registration of pharmaceuticals. Hence, **1** was evaluated in the GLP Ames test, which is designed to detect frame-shift (TA98 and TA1537) and base substitution (TA100 and TA1535) mutations, as well as mutations caused by oxidative stress (*Escherichia coli* $WP_2$uvrA). Compound **1** was not mutagenic in any of the strains tested (± S9; data not shown), except in strain TA1537. There was a shallow dose-dependent reversal of mutation by **1** in the absence of metabolic activation. However, the reversal of mutation did not reach a statistically significant 3-fold increase over the control at all concentrations investigated (Figure 2). In comparison, there was a steeper dose-dependent reversal of mutation by **1** in the presence of metabolic activation. It reached a statistically significant 3-fold increase compared to that of the control only at a dose of 750 $\mu$g/plate (*t* test, $p \leq 0.05$). In both cases, there was a decreased mutation reversal at the top concentration tested, which was attributed to cytotoxicity. This data suggests that a metabolite instead of **1** was responsible for its stronger mutagenic response in TA1537. The positive result in TA1537 was consistent with a frame-shift mutagen, and the frame-shift mutation can be caused by intercalation and/or covalent modification of DNA.[10−12] Two concept analogues designed to overcome genotoxicity included compound **2** (2,5-dimethyl-pyrrolidin-1-yl analogue) and compound **3** (pyridin-3-yl analogue) were tested in the same GLP Ames assay. Interestingly, these gave no dose-dependent increase in mutation reversal in any of the 5 bacterial strains tested, either with or without metabolic activation. Only data from TA1537 is displayed in Figure 2 for comparison across 3 compounds. Therefore, compounds **2** and **3** were not mutagenic in the reverse mutation Ames test.

[$^{3}$H]-**1** (Figure 1) was prepared by adaptation of previously reported 1-step iridium catalyzed *ortho* hydrogen−tritium exchange reaction at the 4-phenyl moiety of **1**.[13] Briefly, a solution of **1** in dichloromethane containing 20 mol % [(cod)Ir(PPF)]$PF_6$ (PPF = [(1*R*)-1-[*bis*(4-methoxy-3,5-dimethylphenyl)phosphino]-2-[(1*R*)-1-(dicyclohexylphosphino)ethyl]-ferrocene] was stirred under 1 atmospheric pressure of tritium gas for 3 h. This tritiated analogue was used to elucidate the mechanism of genotoxicity of **1** from metabolism-dependent covalent binding of [$^{3}$H]-**1** to calf thymus DNA. There was about 12- and 28-fold greater covalent binding to DNA from the incubation of [$^{14}$C]-benzo[*a*]pyrene with induced rat liver S9 in the presence of NADPH over incubation without NADPH or incubation without both S9 and NADPH (Table 1). This data are consistent with those previously reported describing the metabolism-dependent covalent binding of [$^{14}$C]-benzo[*a*]pyrene to DNA.[14] Therefore, this compound was included as a positive control during DNA covalent binding experiments. Similar incubation of DNA with [$^{3}$H]-**1** in NADPH-fortified induced rat liver S9 provided approximately 14- and 18-fold more covalent binding to DNA compared to a similar incubation without NADPH or incubation without NADPH and S9. Hence, incubation of

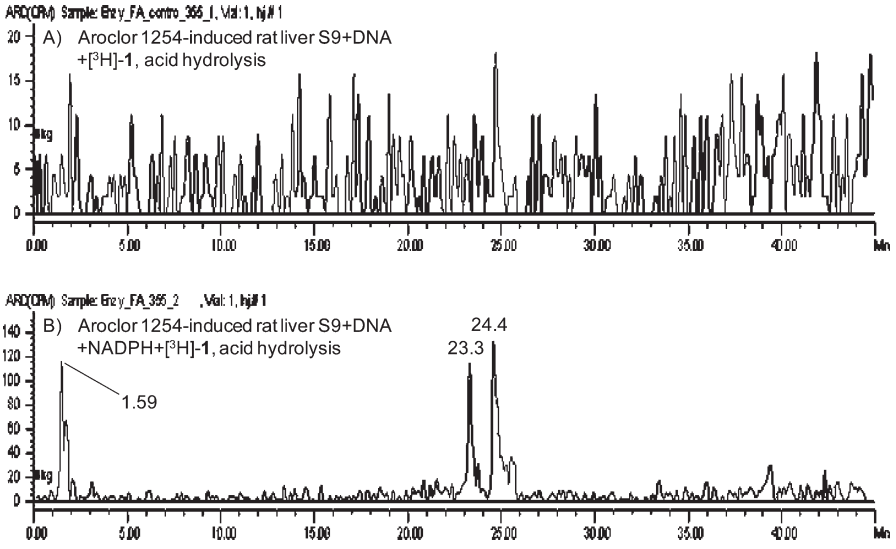


**Figure 3.** Radiochromatograms corresponded to acid hydrolysis of DNA, which had been incubated at 37 °C for 2 h in (A) Aroclor 1254-induced rat liver S9 supplemented with 100 $\mu$M **1** (97.3 $\mu$M **1** + 2.7 $\mu$M [$^3$H]-**1**) and (B) Aroclor 1254-induced rat liver S9 supplemented with 100 $\mu$M **1** (97.3 $\mu$M **1** + 2.7 $\mu$M [$^3$H]-**1**) and NADPH. Analyses were as described in the Experimental Procedures section on LC-RAD-MS analysis.

[$^3$H]-**1** at equimolar concentration gave about 5-fold lower covalent binding to DNA compared to that of [$^{14}$C]-benzo[*a*]pyrene. This covalent binding to DNA was also observed upon replacement of rat with human liver S9 in the presence of NADPH. This was indicated by an approximately 5-fold increase in bound [$^3$H]-**1** related material to DNA relative to that in a similar incubation which used boiled liver S9.

The reactive intermediate responsible for the metabolism-dependent covalent binding of [$^3$H]-**1** to DNA was elucidated indirectly from an incubation of well-established nucleophiles with [$^3$H]-**1** in NADPH-fortified induced rat liver S9. Co-incubation with cyanide ion and methoxylamine resulted in about 58% and 46% reduction in covalent binding of [$^3$H]-**1** to DNA, respectively, compared to the negligible effect by glutathione. However, there was near complete inhibition of the covalent binding of [$^3$H]-**1** to DNA following incubation with both cyanide ion and methoxylamine. The approximate 95% reduction in the covalent binding of [$^3$H]-**1** to DNA is consistent with an additive effect of cyanide ion and methoxylamine. It was speculated that the reduction in covalent DNA binding was unlikely due to the inhibition of metabolism of **1** by either cyanide ion or methoxylamine. Instead, the nucleophile was speculated to compete with DNA for the covalent binding with reactive intermediates of **1**. This is because the NADPH-dependent turnover of 100 $\mu$M **1** in Aroclor 1254-induced rat liver S9 was not significantly inhibited by the addition of either cyanide ion or methoxylamine, or from both nucleophiles (data not shown). This is rather unexpected because of the reported *in vitro* inhibition of rabbit[15] and rat[16] liver microsomal metabolism by cyanide ion. However, the human liver microsomal metabolism was not inhibited by cyanide ion but by methoxylamine.[17] No plausible explanation could be given for the discrepancy except that the current investigations used liver S9 instead of microsomes. These data pointed to the potential involvement of hard electrophiles such as the iminium ion and aldehyde reactive intermediates in the metabolism-dependent covalent binding of [$^3$H]-**1** to DNA.

The direct elucidation of the reactive intermediate involved in covalent binding to DNA was first investigated using a reported procedure for enzymatic hydrolysis of covalently modified DNA to modified 2′-deoxynucleosides.[5] Only one very polar and low abundance radioactive peak (1.59 min) was detected following enzymatic hydrolysis relative to a control sample where NADPH was omitted (data not shown). This polar peak accounted for about 84% of the total radioactivity recovered from the enzymatic hydrolysis of covalently modified DNA. However, the structure of this early eluting radioactive peak was not readily obvious due to the complexity of the full scan mass spectrum because of its elution close to the void volume of the column. An alternative method was therefore used for direct elucidation of the reactive intermediate bound to DNA. This was based on acid hydrolysis of covalently modified DNA to modified nucleobases.[6] Acid hydrolysis of covalently modified DNA, resulting from an incubation of [$^3$H]-**1** with NADPH-fortified induced rat liver S9, provided two radioactive peaks with retention times close to those of **1** (∼17%) and its −2 Da metabolite (∼30%) (Figure 3B). In addition, a radioactive peak (1.59 min, ∼18%) was also detected close to the retention time as the peak from enzymatic hydrolysis. These 3 peaks were not detected from acid hydrolysis of the control sample (Figure 3A). Together, they accounted for about 65% of bound [$^3$H]-**1**-related materials released from acid hydrolysis of the modified DNA. It was speculated that tritium exchanged during acid hydrolysis by an unknown mechanism may be responsible for this observed lower than expected recovery of total radioactivity. The later eluting radioactive peaks at retention times of 23.3 and 24.4 min have molecular weights of 356 and 354 Da, which is identical to that of **1** and its enamine metabolite, respectively (see Supporting Information for the identification of the enamine metabolite). Both **1** and its enamine metabolite produced an identical base peak at *m*/*z* 286 upon CID of its respective protonated molecule ([M + H]$^+$) (data not shown), and the assignment of *m*/*z* 286 will be described in the section on elucidation of cyano conjugates structures. The detection of **1** and its enamine metabolite instead of a nucleobase adduct may be due to the instability of the nucleobase adduct under acidic hydrolysis conditions. However, no rationalization can be offered for the release of **1** and its

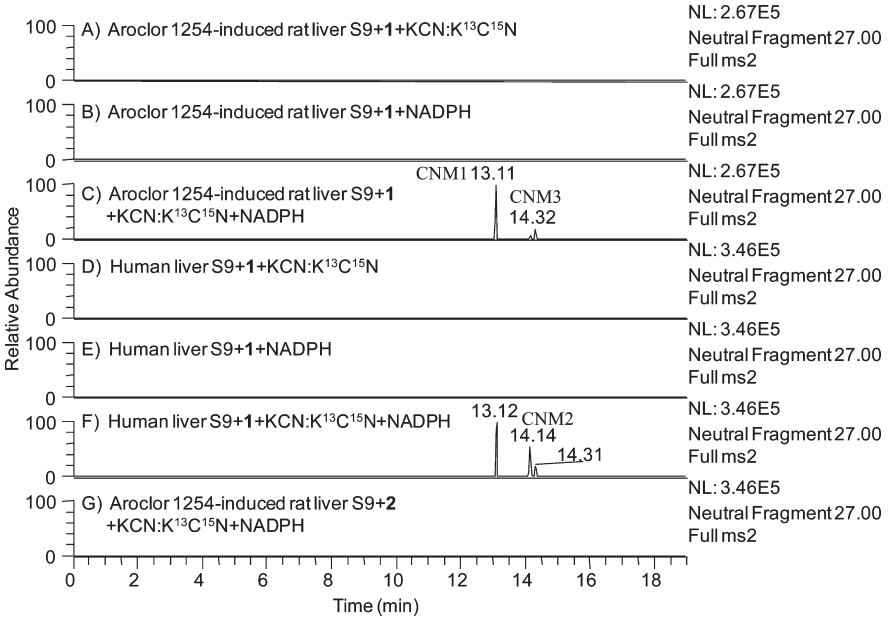


**Figure 4.** Reconstructed ion chromatogram (RIC) corresponding to the neutral mass loss of 27 Da from isotopic pattern triggered data-dependent mass analysis of the incubation of 100 $\mu$M **1** at 37 °C for 1 h in (A) Aroclor 1254-induced rat liver S9 supplemented with 2:1 ratio KCN:$K^{13}C^{15}N$, (B) Aroclor 1254-induced rat liver S9 supplemented with a NADPH regenerating system, (C) Aroclor 1254-induced rat liver S9 supplemented with both 2:1 ratio KCN:$K^{13}C^{15}N$ and a NADPH regenerating system, (D) human liver S9 supplemented with 2:1 ratio KCN/$K^{13}C^{15}N$, (E) human liver S9 supplemented with a NADPH regenerating system, and (F) human liver S9 supplemented with both 2:1 ratio KCN:$K^{13}C^{15}N$ and a NADPH regenerating system. RIC corresponded to the neutral mass loss of 27 Da from an analysis of incubation of 100 $\mu$M **2** in Aroclor 1254-induced rat liver S9 supplemented with both 2:1 ratio KCN:$K^{13}C^{15}N$ and a NADPH regenerating system (G).

enamine metabolite during acid hydrolysis of the modified DNA. Perhaps trapping of reactive metabolite(s) with nucleobases followed by investigation of its stability under acidic conditions may provide insight into the release of tritiated products, especially **1**.

The direct elucidation of the structure of the reactive intermediate was not successful by either enzymatic or acid hydrolysis of the covalently modified DNA. Hence, the structure of the reactive intermediate covalently bound to DNA was inferred indirectly from trapping experiments with well-established chemical nucleophiles as described in the sections to follow.

**Trapping Iminium Ions Reactive Intermediates as Cyano Conjugates.** The observation that cyanide ion trapping affords protection against the covalent binding of **1** to DNA is suggestive of **1** undergoing bioactivation to form iminium ions reactive intermediates. The structure elucidation of iminium ions typically involved LC-MS analysis of cyano conjugates[18] and was similarly deployed in our investigations. Isotopic pattern mass filtering of full scan accurate mass data for cyano conjugates was conducted using an exact mass delta of 2.00039 Da and an isotope ratio of 0.52 or 0.97.[7] Three potential cyano conjugates were detected from the incubation of **1** with induced rat liver S9 containing an NADPH-regenerating system and a 2:1 ratio of KCN:$K^{13}C^{15}N$ (data not shown). These 3 cyano conjugates with a retention time relative to the unchanged drug (RRT) of 1.13 (CNM1: $[M + H]^+ = m/z$ 396), 1.22 (CNM2: $[M + H]^+ = m/z$ 407), and 1.24 (CNM3: $[M + H]^+ = m/z$ 407) min were also detected in the reconstructed ion chromatogram (RIC) resulting from filtering $MS^2$ data by neutral mass loss of 27 Da as shown in Figure 4C. The neutral mass loss of 27 Da (HCN) upon CID is diagnostic of cyano conjugates.[18] These cyano conjugates were only formed from the incubation of **1** with induced rat liver S9 supplemented with a 2:1 ratio of KCN:$K^{13}C^{15}N$ and a NADPH-regenerating system (Figure 4A–C). This NADPH-dependent formation of cyano conjugates provided evidence for the metabolic bioactivation of **1** to iminium ions. All three cyano conjugates were also detected from incubations of **1** in Aroclor 1254-induced rat liver microsomes (data not shown) or in human liver S9 fortified with the NADPH-regenerating system and a 2:1 ratio of KCN:$K^{13}C^{15}N$ (Figure 4D–F). They were again absent in a similar incubation which omitted either the NADPH-regenerating system (Figure 4D) or the 2:1 ratio of KCN:$K^{13}C^{15}N$ (Figure 4E). The UV absorption spectrum of each cyano conjugate was characterized by $\lambda_{max}$ at 228, 308, and 350 nm. However, the highest sensitivity was obtained from displaying the UV chromatogram at a $\lambda_{max}$ of 308 nm, and the peak area mentioned hereafter corresponded to $\lambda_{max}$ of 308 nm. Therefore, a comparison of peak areas gave an approximate 4-, 2-, and 2-fold greater formation of cyano conjugates CNM1, CNM2, and CNM3, respectively, by Aroclor 1254-induced rat liver S9 compared to liver microsomes. Furthermore, no cyano conjugate was detected from the incubation of **2** under conditions identical to those of **1** (Figure 4G), which was designed to minimize bioactivation to iminium ions. The site of bioactivation was determined from the localization of site of attachment of the cyanide ion to **1** by high resolution data-dependent accurate mass measurements.

High resolution accurate mass measurement of the $[M + H]^+$ of the cyano conjugate, CNM1, gave a chemical formula of $C_{23}H_{18}N_5O_2$ (17.5 rings plus double-bonds [RDB], −0.03 ppm) from the exact $m/z$ 396.14549 (Figure 5A). Comparison of the chemical formula with that of **1** suggested that CNM1 was a cyano conjugate of pyrrolidinone-**1** (Figure 5A and C). CID of the $[M + H]^+$ gave a product ion at $m/z$ 369.13464 ($C_{22}H_{17}N_4O_2$, 16.5RDB,

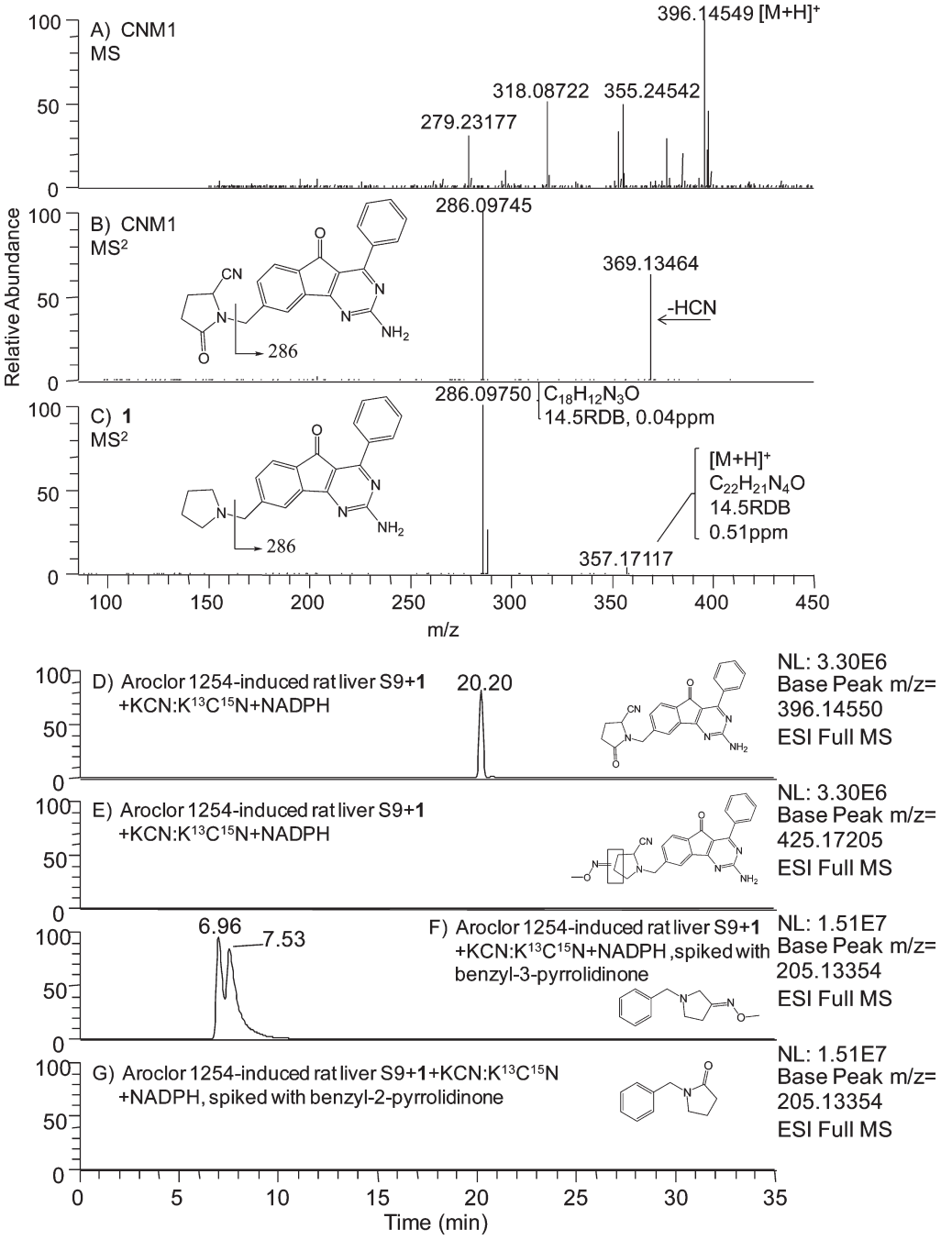


**Figure 5.** Full scan (A) and product ion (B) accurate mass spectra of cyano conjugate CNM1 detected at 13.11 min in Figure 4C from isotopic pattern triggered data-dependent accurate mass analysis of the incubation of 100 $\mu$M **1** at 37 °C for 1 h in Aroclor 1254-induced rat liver S9 supplemented with both 2:1 ratio KCN:$K^{13}C^{15}N$ and a NADPH regenerating system. The product ion accurate mass spectrum of **1** (C) was included to facilitate the assignment of product ions of CNM1. The localization of the position of the carbonyl group in the pyrrolidine moiety of **1** was by derivatization with methoxylamine and pyridine. Oxime derivatives were analyzed using a greater chromatographic resolution LC-MS method as described in the Experimental Procedures section. RIC corresponding to theoretical *m/z* of 2-cyano-5-pyrrolidinone-**1** (D) and the oxime derivative of 2-cyano-keto-**1** (E) following derivatization of CNM1 in the above incubate with methoxylamine and pyridine. RIC from the derivatization of 10 $\mu$M each of benzyl-3-pyrrolidinone (keto) (F) or benzyl-2-pyrrolidinone ($\gamma$-lactam) (G) spiked in the above incubate with methoxylamine and pyridine.

0.10 ppm) from the loss of a neutral HCN molecule and corroborated that CNM1 was indeed a cyano conjugate (Figure 5B). In addition, it gave the same product ion at *m/z* 286.09745 ($C_{18}H_{12}N_3O$, 14.5RDB, −0.14 ppm) as that from **1**, which confirmed that the 2-amino-8-methyl-4-phenyl-indeno[1,2-d]pyrimidin-5-one (hereafter referred to as 8-methyl-arylindenopyrimidine) part of **1** was intact (Figure 5B and C). This suggested that the pyrrolidine ring was the site of modification, which included the addition of a cyanide ion to the α-carbon atom and localization of the carbonyl functionality to either the α- or $\beta$-position.

The position of the carbonyl group in the pyrrolidine ring of CNM1 was established by attempting to form an oxime


dx.doi.org/10.1021/tx1004437 |*Chem. Res. Toxicol.* 2011, 24, 1012–1030

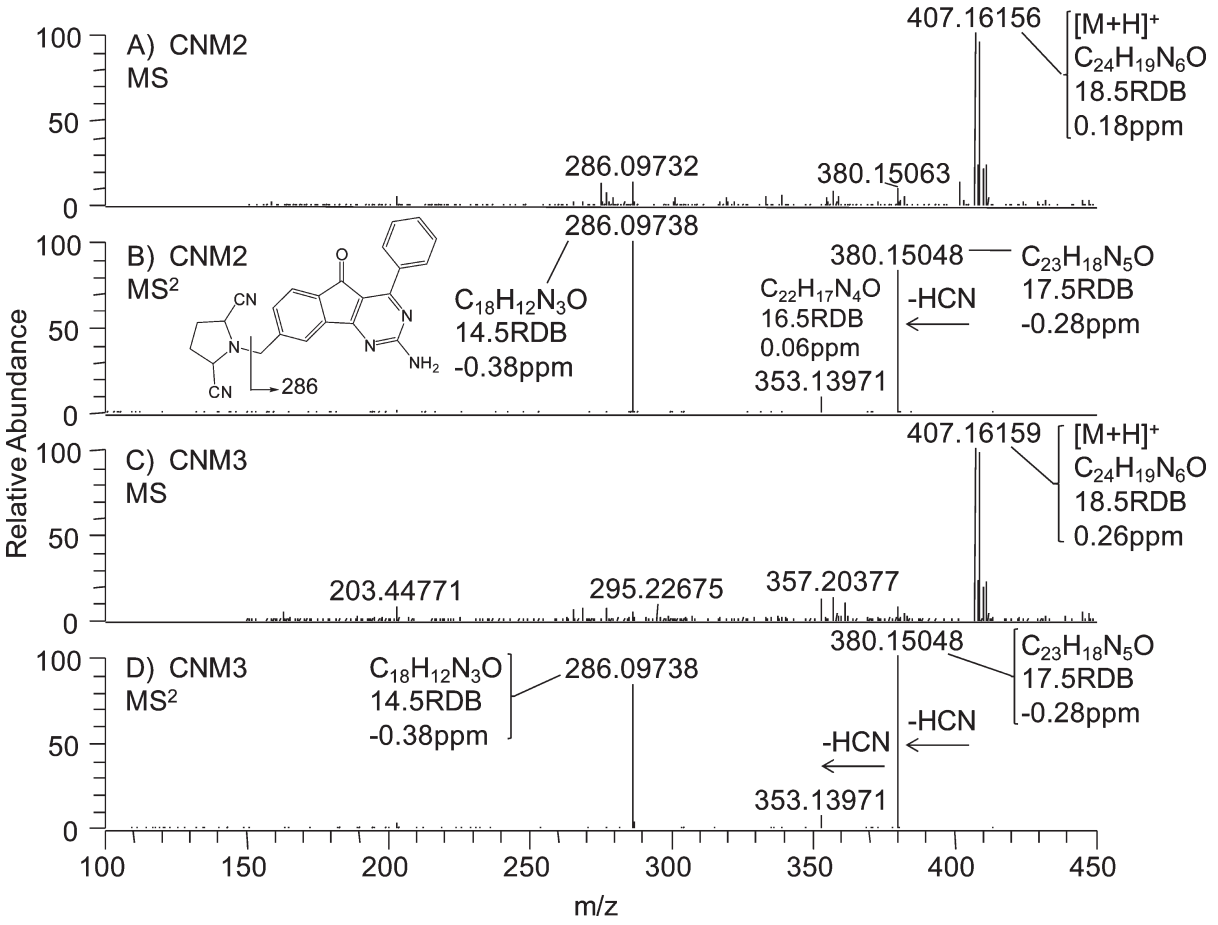


**Figure 6.** Full scan (A) and product ion (B) accurate mass spectra of the 2,5-dicyano conjugate CNM2 detected at 14.16 min in Figure 4C from isotopic pattern triggered data-dependent accurate mass analysis of an incubation of 100 $\mu$M **1** at 37 °C for 1 h in Aroclor 1254-induced rat liver S9 supplemented with both 2:1 ratio KCN:$K^{13}C^{15}N$ and a NADPH regenerating system. Full scan (C) and product ion (D) accurate mass spectra of the 2,5-dicyano conjugate CNM3 at 14.32 min in Figure 4C from an analysis of the same incubation mixture.

derivative using methoxylamine.[9] This identification is made possible because the arylindenopyrimidinyl carbonyl group and the α-carbonyl group of the pyrrolidine ring of CNM1 do not form oxime derivatives with methoxylamine. It is speculated that steric hindrance is the main reason for the lack of reactivity of the arylindenopyrimidinyl carbonyl group with methoxylamine. The derivatization of the NADPH- and KCN-fortified induced rat liver S9 incubate of **1** did not form an oxime derivative of CNM1 as indicated by the absence of a chromatographic peak in RIC corresponding to theoretical *m/z* of the oxime derivative of 2-cyano-3- or 4-pyrrolidinone-**1** at 425.17205 (Figure 5E). Also, there was little change to the peak area of the underivatized CNM1 at 20.20 min in the RIC of theoretical *m/z* 396.14550 (Figure 5D). The lack of derivatization of CNM1 was not due to insufficient methoxylamine since there was derivatization of benzyl-3-pyrrolidinone when spiked into an identical incubation of **1**. This was supported via the detection of a pair of chromatographic peaks at 6.96 and 7.53 min with *m/z* 205.13335 (5.5RDB, −0.93 ppm) and 205.13337 (5.5RDB, −0.83 ppm), respectively, in Figure 5F. These measured masses gave identical chemical formulas of $C_{12}H_{17}N_2O$ and product ion mass spectra, which were consistent with the E and Z isomers of oxime derivatives of benzyl-3-pyrrolidinone (data not shown). However, there was no derivatization of benzyl-2-pyrrolidinone when spiked into an identical incubation of **1** as indicated by the absence of a chromatographic peak in identical RIC (Figure 5G). The derivatization behavior of CNM1 resembled that of benzyl-2-pyrrolidinone. Therefore, this suggested a structure of 2-cyano-5-pyrrolidinone-**1** for CNM1 since the γ-lactam's carbonyl group was not known to be reactive toward methoxylamine.[9]

The protonated molecules of CNM2 and CNM3 at exact *m/z* 407.16156 (18.5RDB, 0.18 ppm) and 407.16159 (18.5RDB, 0.26 ppm), respectively, resulted in an identical chemical formula of $C_{24}H_{19}N_6O$ (Figure 6A and C). This chemical formula suggested the introduction of 2 cyano groups into **1**. This was corroborated by the sequential diagnostic loss of HCN to form the product ions at *m/z* 380.15048 ($C_{23}H_{18}N_5O$, 17.5RDB, −0.28 ppm) and 353.13971 ($C_{22}H_{17}N_4O$, 16.5RDB, 0.06 ppm) from the CID of the $[M + H]^+$ of CNM2 (Figure 6B) or CNM3 (Figure 6D). The loss of 2 molecules of HCN was consistent with a dicyano conjugate. The product ion at *m/z* 286.09738 ($C_{18}H_{12}N_3O$, 14.5RDB, −0.38 ppm) provided evidence for the unchanged 8-methyl-arylindenopyrimidine moiety and the presence of the 2,5-dicyanopyrrolidine ring. The product ion mass spectra of CNM2 and CNM3 were essentially similar except for the relative abundances of their product ions (Figure 6B and D). This suggests the sequential addition of a cyanide ion to each α-carbon atom of the endocyclic iminium ion of **1** resulting in the formation of cis and trans geometric isomers and diastereomers of 2,5-dicyanopyrrolidinyl-**1**. This further explained its

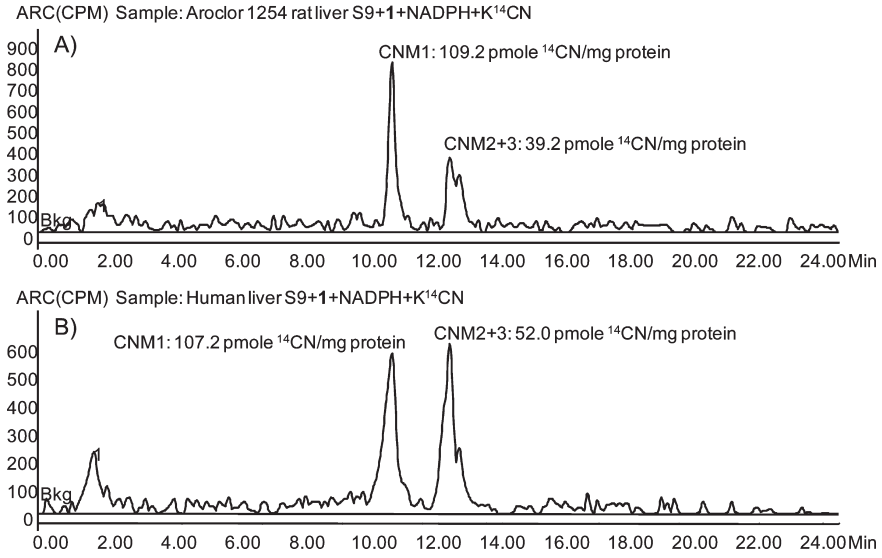


**Figure 7.** Radiochromatograms corresponding to cyano conjugates CNM1−3 from simultaneous radioprofiling and a mass spectrometric analysis of the incubation of 100 $\mu$M **1** in (A) Aroclor 1254-induced rat liver S9 supplemented with both KCN: $K^{13}C^{15}N+K^{14}CN$ and a NADPH regenerating system, and (B) human liver S9 supplemented with both KCN:$K^{13}C^{15}N+K^{14}CN$ and a NADPH regenerating system. All analyses were as described in the Experimental Procedures section on LC-RAD-MS analysis.

chromatographic separation on an achiral column. However, the exact stereochemistry of the 2,5-dicyanopyrrolidinyl-**1** was not assigned in this study.

The metabolic pathways leading to the formation of these cyano conjugates and enzyme(s) catalyzing these pathways were investigated. There was no 2-cyanopyrrolidinyl-**1** detected at 1-h incubation or at shorter incubation times of 30, 15, 10, or 5 min. Therefore, it was difficult to provide evidence to support further metabolism of 2-cyanopyrrolidinyl-**1** to either 2-cyano-5-pyrrolidinone-**1** (CNM1) or 2,5-dicyanopyrrolidinyl-**1** (CNM2 and CNM3). Also, no 2-cyano-5-pyrrolidinone-**1** was formed from the incubation of 1 $\mu$M isolated $\gamma$-lactam metabolite of **1** under similar conditions used for trapping iminium ions (data not shown). The structural elucidation of the $\gamma$-lactam metabolite of **1** will be described in Supporting Information.

Similar incubations employing approximately 0.2 $\mu$M of isolated cis and trans 2,5-dicyanopyrrolidinyl-**1** (CNM2 and CNM3) were performed without the cyanide ion. There was extensive metabolism of the 2,5-dicyano conjugate by NADPH-fortified Aroclor 1254-induced rat liver S9 since no 2,5-dicyano conjugates remained after 1 h of incubation (Supporting Information Figure 1B). A cyano conjugate was, however, detected with similar retention time as that of CNM1 (Supporting Information Figure 1B and C), and the product ion mass spectrum was consistent with the formation of 2-cyano-5-pyrrolidinone-**1** (data not shown). The formation of 2-cyano-5-pyrrolidinone-**1** from the 2,5-dicyano conjugates was NADPH-dependent since this cyano conjugate was not detected from similar incubation in the absence of NADPH (Supporting Information Figure 1A). The formation of only 2-cyano-5-pyrrolidinone-**1** from incubation with the 2,5-dicyano conjugates provided additional evidence that CNM2 and CNM3 are indeed geometric isomers of 2,5-dicyanopyrrolidinyl-**1**. Furthermore, the formation of 2-cyano-5-pyrrolidinone-**1** was inhibited by an average of 89% (range: 88, 89%) by 100 $\mu$M SKF-525A and an average of 91% (range: 91, 92%) by 100 $\mu$M menadione from coincubation under similar conditions with 10 $\mu$M of **1**. The data provided evidence for the metabolism of 2,5-dicyanopyrrolidinyl-**1** to 2-cyano-5-pyrrolidinone-**1**. Also, the inhibition of 2-cyano-5-pyrrolidinone-**1** formation by menadione is suggestive of an alternate metabolic route for its formation.

**Quantification of Iminium Ions as [$^{14}$C]-Cyano Conjugates.** The amounts of total iminium ions formed from the incubation of **1** in Aroclor 1254-induced rat and human liver S9, in the presence of a NADPH regenerating system and [$^{14}$C]-cyanide ion, were determined to be approximately 0.3% of **1** (Figure 7). The incubation of **1** in NADPH-fortified Aroclor 1254-induced rat liver S9 resulted in the formation of about 109 and 39 pmol equivalents/mg protein of 2-cyano-5-pyrrolidinone-**1** (CNM1) and 2,5-dicyanopyrrolidinyl-**1** (CNM2 + CNM3) conjugates, respectively. Comparable amounts of cyano conjugates were produced (~107 [CNM1] and ~52 [CNM2 + CNM3] pmol equivalents/mg protein) in a human liver S9 preparation.

**Trapping of Aldehyde Reactive Intermediates as the Oxime Conjugates.** The addition of methoxylamine also led to protection against the covalent binding of **1** to DNA, which is consistent with the bioactivation of **1** to reactive aldehyde intermediates. The formation of reactive aldehyde intermediates from **1** was investigated by the incubation of **1** in NADPH-fortified Aroclor 1254-induced rat liver S9 in the presence of a 2:1 ratio of methoxylamine/methoxyl-$d_3$-amine. Reactive aldehyde intermediates were detected as oxime conjugates following the reaction of the reactive aldehyde functionality with methoxylamine.

The oxime conjugates were detected by interrogation of full scan accurate mass data by isotopic pattern filtering using an exact mass delta of 3.01883 and an isotopic ratio of 0.4. Two oxime conjugates were detected at an RRT of 1.40 (OM1) and 1.45 (OM2) with an isotopic doublet ($[M + H]^+$) at $m/z$ 331.11804 ($C_{19}H_{15}N_4O_2$, 14.5RDB, −2.76 ppm):334.13680 ($C_{19}H_{12}{}^2H_3N_4O_2$, 14.5RDB, −2.94 ppm) and 331.11816 ($C_{19}H_{15}N_4O_2$, 14.5RDB, −2.45 ppm):334.13694 ($C_{19}H_{12}{}^2H_3N_4O_2$, 14.5RDB, −2.52 ppm), respectively (Figure 8A and C). CID of $[M + H]^+$ of the oxime conjugate OM1 gave a base peak at $m/z$ 273.08929 ($C_{17}H_{11}N_3O$, 14.0RDB, −1.37 ppm),

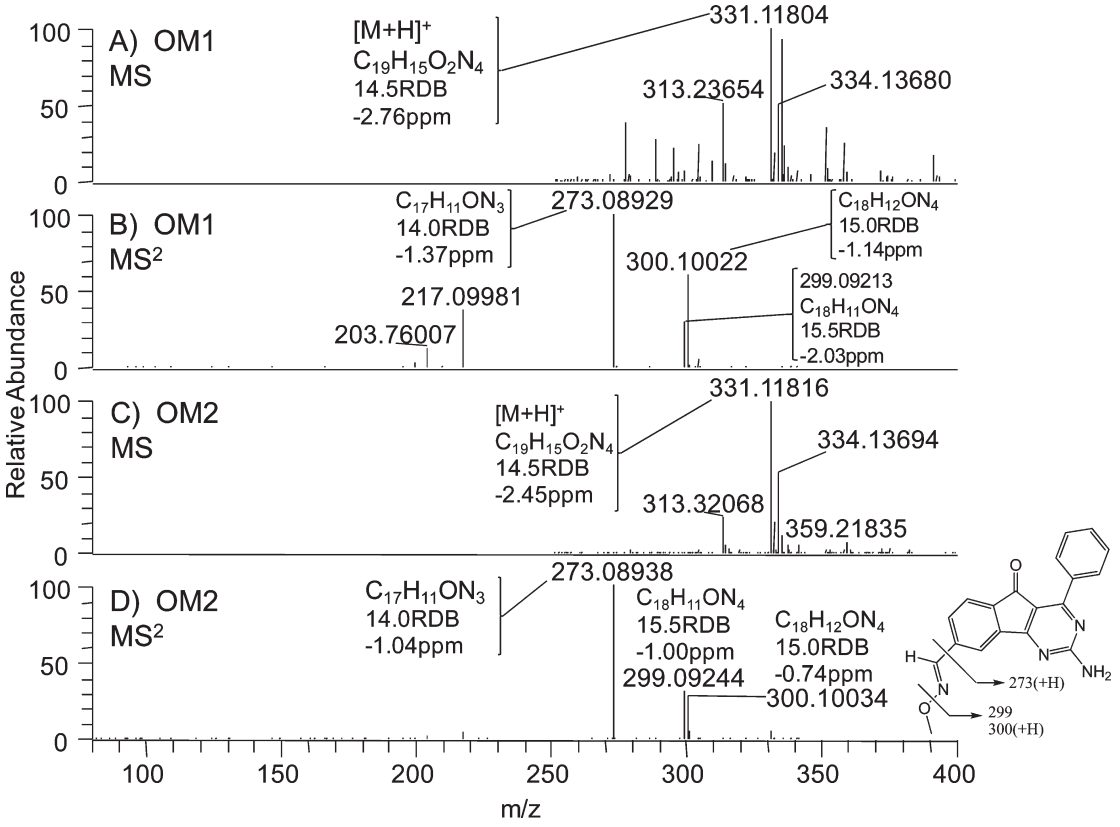


**Figure 8.** Full scan and product ion accurate mass spectra of oxime conjugates OM1 (A, B) and OM2 (C, D) detected from isotopic pattern triggered data-dependent accurate mass analysis of incubation of 100 $\mu$M **1** in Aroclor 1254-induced rat liver S9 supplemented with a 2:1 ratio of methoxylamine/methoxyl-$d_3$-amine and a NADPH regenerating system. Oxime conjugates in reconstituted samples were analyzed using a greater chromatographic resolution LC-MS method as described in the Experimental Procedures section. Orbitrap was calibrated using an ES-TOF tuning mix (Agilent, Santa Clara, CA) immediately prior to mass measurements under external calibration mode.

which was consistent with the unchanged 2-amino-4-phenyl-indeno-[1,2-*d*]pyrimidin-5-one moiety of **1** (Figure 8B). A pair of product ions at *m/z* 299.09213 ($C_{18}H_{11}N_4O$, 15.5RDB, −2.03 ppm) and 300.10022 ($C_{18}H_{12}N_4O$, 15.0RDB, −1.14 ppm) were rationalized to derive from the loss of a $CH_3OH$ molecule and $OCH_3$ radical, respectively, from $[M + H]^+$. These 3 product ions when taken together are consistent with an oxime conjugate of 2-amino-5-oxo-4-phenyl-5*H*-indeno[1,2-*d*]pyrimidine-8-carbaldehyde (hereafter referred to as aldehyde-**1**). The similarity of the product ion mass spectrum of OM2 to that of OM1 suggested that they are probably the E and Z isomers of the oxime conjugates (Figure 8B and D).

The indirect detection of iminium ion intermediates from **1** suggested the presence of downstream ring-opened amino aldehyde metabolite intermediates. However, they were not detected by isotopic pattern filtering of the full scan accurate mass data. The liver microsomal incubates were reanalyzed by a targeted product ion scan of the expected $[M + H]^+$ at *m/z* 402. As a result, two oxime conjugates, OM3 and OM4, at RRTs of 1.07 and 1.12 in the RIC at exact *m/z* 286.09701, were detected from the incubation of **1** only in the presence of methoxylamine and NADPH (Figure 9A and B). The detection of these 2 oxime conjugates only by the product ion scan suggests that they were formed in trace amounts below the limit of detection of full scan mass analysis. The accurate masses of the base peaks at *m/z* 286.09727 and 286.09720 from OM3 and OM4, respectively, gave an identical chemical formula of $C_{18}H_{12}N_3O$. This suggested that the pyrrolidine ring was the site of bioactivation for both conjugates (Figure 9C and D). Another product ion at *m/z* 303.12384 ($C_{18}H_{15}N_4O$, 13.5RDB, −0.65 ppm), which corresponded to protonated 2-amino-8-aminomethyl-4-phenyl-indeno[1,2-*d*]-pyrimidin-5-one, was detected in the product ion mass spectrum of OM4 by accurate mass analysis (data not shown). However, this product ion was only detected in OM3 from nominal mass analysis. This product ion was not detected upon CID of $[M + H]^+$ of compounds with an intact pyrrolidine ring such as **1**, or the cyano conjugates, CNM1, CNM2, and CNM3. It is likely that neither OM3 nor OM4 was the ring-closed isomer since no product ion was detected from the loss of the $NHOCH_3$ moiety. OM3 and OM4 were tentatively assigned the E and Z isomers of the oxime conjugates on the basis of the similarity of their product ion mass spectra.

An additional minor oxime conjugate OM5 (RRT: 1.03), with an isotopic doublet of $[M + H]^+$ at *m/z* 400.17617 ($C_{23}H_{22}O_2N_5$, 15.5RDB, −1.58 ppm) and 403.19497 ($C_{23}H_{19}{}^2H_3O_2N_5$, 15.5RDB, −1.64 ppm), was detected by the isotopic pattern filtering method (Figure 9E). The chemical formula of OM5 ($C_{23}H_{22}O_2N_5$, 15.5RDB) contained 2H and 1 RDB less than those of OM3 or OM4 ($C_{23}H_{24}O_2N_5$, 14.5RDB), which suggested the presence of an unsaturated double bond. CID gave a product ion at *m/z* 286.09671 ($C_{18}H_{23}ON_3$, 14.5RDB, −2.72 ppm), which supported an unchanged 8-methyl-arylindenopyrimidine moiety of **1** (Figure 9F). The base peak at *m/z* 355.15498 resulted in a chemical formula of $C_{22}H_{19}ON_4$ (15.5RDB, −1.01 ppm) which is consistent with the loss of a $NHOCH_3$ moiety and the gain of 2H. Such a loss was more likely

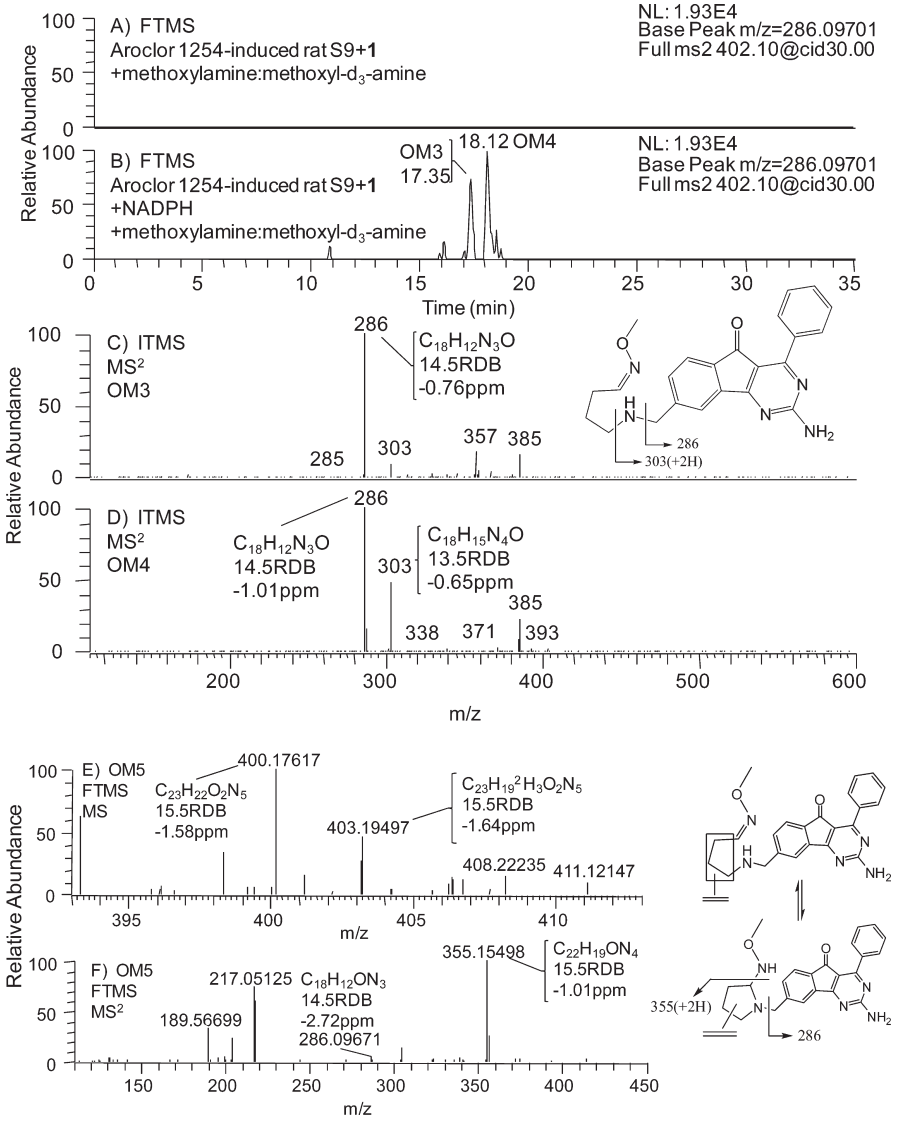


**Figure 9.** RIC corresponding to the base peak at exact $m/z$ 286.09701 from a product ion scan of $[M + H]^+$ of oxime conjugate at $m/z$ 402 following an analysis of incubation of 100 $\mu$M **1** in (A) Aroclor 1254-induced rat liver S9 supplemented with 2:1 ratio methoxylamine/methoxyl-$d_3$-amine, and (B) Aroclor 1254-induced rat liver S9 supplemented with both 2:1 ratio methoxylamine/methoxyl-$d_3$-amine and a NADPH regenerating system. Product ion mass spectra of oxime conjugates OM3 and OM4 detected at retention time of 17.35 min (C) and 18.12 min (D), respectively. Full scan (E) and product ion mass spectrum (F) of a ring-closed oxime conjugate analogue OM5 identified from an incubation of 100 $\mu$M **1** in B. Oxime conjugates in reconstituted samples were analyzed using a greater chromatographic resolution LC-MS method as described in the Experimental Procedures section. Orbitrap was calibrated using an ES-TOF tuning mix (Agilent, Santa Clara, CA) immediately prior to mass measurements under external calibration mode.

to occur in the presence of an amine rather than an imine bond linking the methoxylamine moiety to the pyrrolidine ring. This is corroborated by the absence of this product ion from the bond cleavage of the OM3 and OM4 oxime conjugates. The retention of the same RDB of 15.5 in the base peak at $m/z$ 355.15498 together with the intact 8-methyl-arylindenopyrimidine moiety of **1** suggested the presence of a monounsaturated pyrrolidine ring. Hence, OM5 was tentatively assigned an oxime conjugate of a monounsaturated amino aldehyde metabolite intermediate. The observation of the fragmentation pathway leading to the base peak at $m/z$ 355.15498 favored a ring-closed oxime conjugate for OM5 (Figure 9F). However, the site of unsaturation in the pyrrolidine ring of OM5 could not be established by tandem mass spectrometry.

**Trapping of Soft Electrophilic Reactive Intermediates as Glutathione Conjugates.** Trapping experiments with glutathione (GSH) were conducted to provide rationalization for the ineffectiveness of GSH to reduce the covalent binding of **1** to DNA. The GSH conjugates were detected from the full scan accurate MS data by isotopic pattern filtering using a mass delta of 3.00375 Da and an isotope ratio of 0.43. As a result, 3 GSH conjugates were detected following the incubation of **1** in Aroclor 1254-induced rat liver S9 containing an NADPH-regenerating system and a 2:1 ratio of GSH:[$^{13}C_2{}^{15}$N-gly]GSH (data not shown). The formation of these three GSH conjugates was NADPH-dependent. The GSH conjugates at RRT of 0.78, 0.86, and 0.97 have accurate $[M + H]^+$ at $m/z$ 694.22975 (GSM1: $C_{32}H_{36}O_9N_7S$, 18.5RDB, 1.12 ppm), 694.22926


dx.doi.org/10.1021/tx1004437 |Chem. Res. Toxicol. 2011, 24, 1012–1030

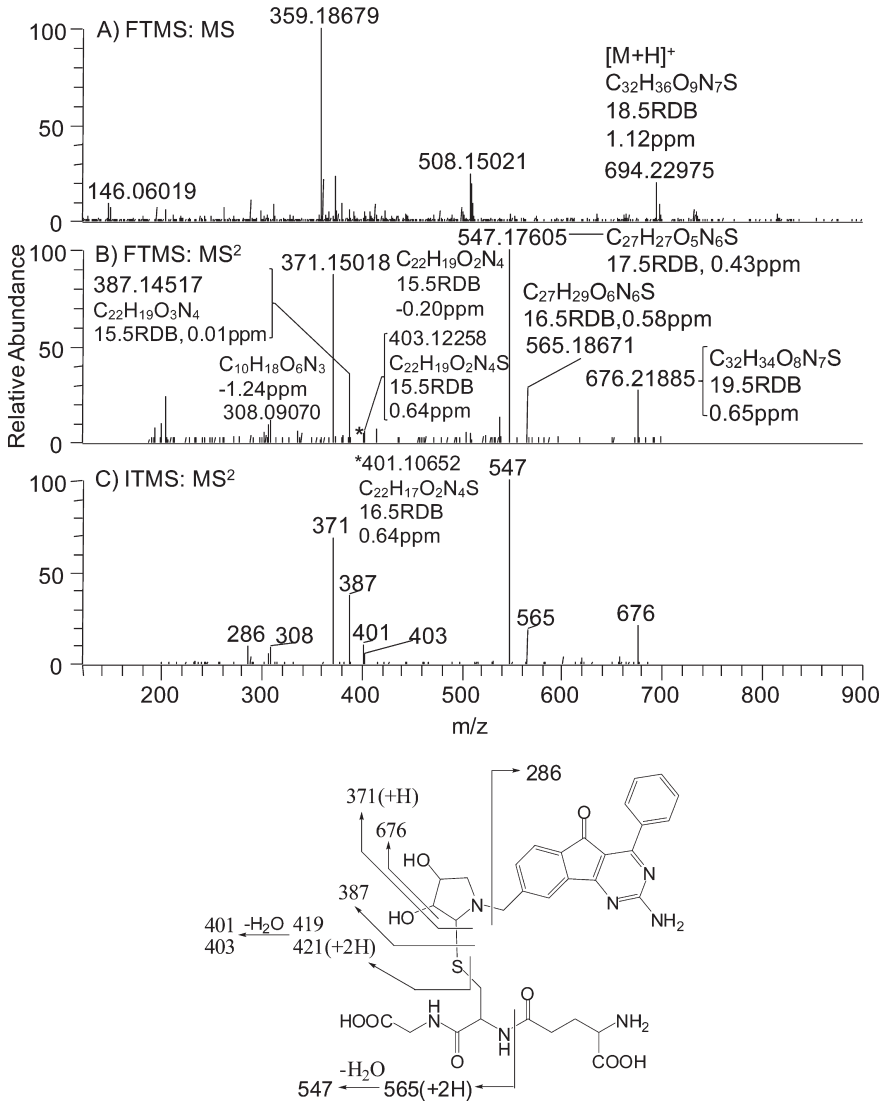


**Figure 10.** Full scan (A) and product ion (B) accurate mass spectra of the proposed hypothetical structure of the glutathione conjugate GSM1 (an isomer of GSM2) detected by isotopic pattern triggered data-dependent accurate mass analysis of incubation of 100 $\mu$M **1** in Aroclor 1254-induced rat liver S9 supplemented with 2:1 ratio GSH:[$^{13}C_2{}^{15}N$-gly]GSH and a NADPH regenerating system. The product ion nominal mass spectrum of GSM1 acquired to show the presence of low abundance product ion at $m/z$ 286 (C).

(GSM2: $C_{32}H_{36}O_9N_7S$, 18.5RDB, 0.41 ppm), and 676.21870 (GSM3: $C_{32}H_{34}O_8N_7S$, 19.5RDB, 0.43 ppm), respectively (Figures 10−12). The chemical formulas of $C_{32}H_{36}O_9N_7S$, $C_{32}H_{36}O_9N_7S$, and $C_{32}H_{34}O_8N_7S$ were consistent with the compositions of (**1**+GSH+$O_2$-2H), (**1**+GSH+$O_2$-2H), and (**1**+GSH+O-4H), respectively. The glutathione composition of (**1**+GSH+$O_2$-2H) and (**1**+GSH+O-4H) were postulated to correspond to glutathion-*S*-yl-dioxy-pyrrolidinyl-**1** and glutathion-*S*-yl-pyrrolidinone-**1**, respectively.

All three conjugates displayed neutral mass losses diagnostic of GSH conjugates[19] upon CID of their respective $[M + H]^+$. These included losses of pyroglutamic acid (minus 129 Da; GSM1 and 2: $m/z$ 565 [$C_{27}H_{29}O_6N_6S$]; GSM3, $m/z$ 547 [$C_{27}H_{27}O_5N_6S$]) and the GSH molecule (minus 307 Da; GSM1 and 2, $m/z$ 387 [$C_{22}H_{19}O_3N_4$]; GSM3, 369 [$C_{22}H_{17}O_2N_4$]). The ion at $m/z$ 286 in the product ion mass spectra of all GSH conjugates provided evidence for an intact 8-methyl-arylindenopyrimidine moiety. This suggested that the pyrrolidine ring was the site of bioactivation for these GSH conjugates. GSM1 and GSM2 are isomeric GSH conjugates based on the identical chemical formulas of their $[M + H]^+$ and identical product ions at $m/z$ 286, 371, 387, 401, 403, 547, 565, and 676. Further isolation of $m/z$ 387 for CID did not eliminate the elemental oxygen to form the product ion at $m/z$ 371 ($C_{22}H_{19}O_2N_4$). Hence, it is unlikely that oxygen atom addition to the pyrrolidine nitrogen atom occurs (data not shown). Instead, this product ion ($m/z$ 371) is rationalized to derive from 4-center rearrangement involving vicinal hydroxy and GSH groups followed by the transfer of one H for either GSM1 (Figure 10) or GSM2 (Figure 11). This facile loss of a molecule of water to give the base peak at $m/z$ 676 for GSM2 compared to its lower abundance for GSM1 is due to the greater gaseous phase stability of the iminium ion over the secondary carbocation. This explanation also accounted for the higher relative abundance of the product ion at nominal $m/z$ 387 for GSM1. Hence, the conjugate with glutathione added to the α-carbon atom of the pyrrolidine ring would be expected to display


dx.doi.org/10.1021/tx1004437 |*Chem. Res. Toxicol.* 2011, 24, 1012–1030

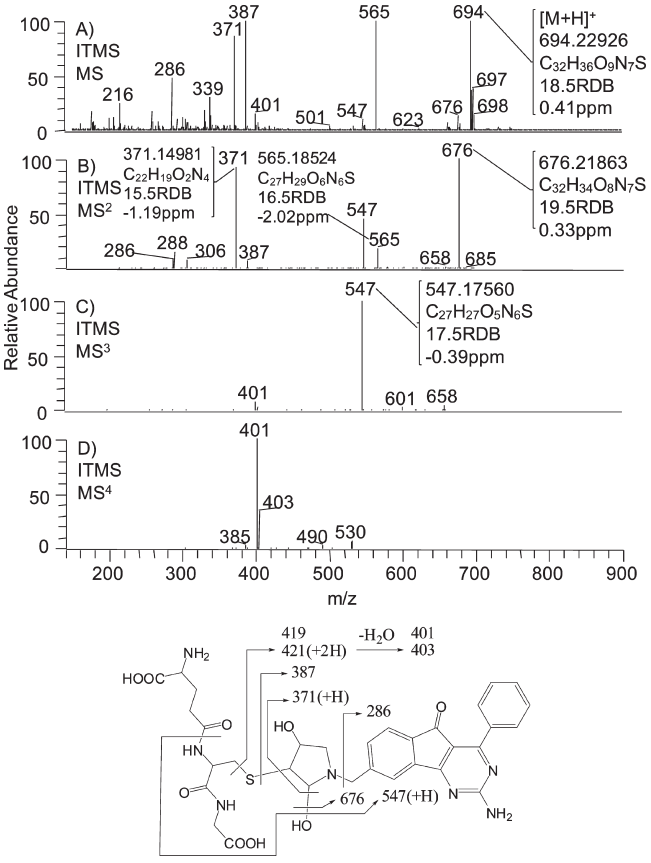


**Figure 11.** Full scan (A) and product ion (B, C, and D) nominal mass spectra of the proposed hypothetical structure of the glutathione conjugate GSM2 detected by isotopic pattern triggered data-dependent nominal mass analysis of incubation of 100 $\mu$M **1** in Aroclor 1254-induced rat liver S9 supplemented with 2:1 ratio GSH:[$^{13}C_2{}^{15}N$-gly]GSH and a NADPH regenerating system. Accurate $m/z$ and chemical formulas of selected product ions were included from accurate mass measurements on the Orbitrap.

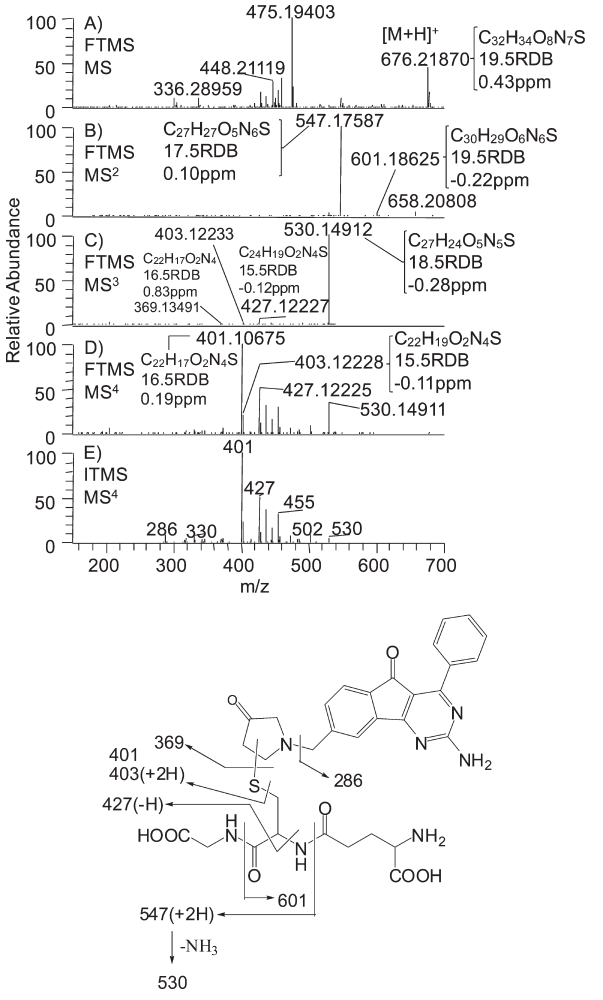


**Figure 12.** Full scan (A) and product ion (B−D) accurate mass spectra of the proposed hypothetical structure of the glutathione conjugate GSM3 detected by isotopic pattern triggered data-dependent accurate mass analysis of incubation of 100 $\mu$M **1** in Aroclor 1254-induced rat liver S9 supplemented with 2:1 ratio GSH:[$^{13}C_2{}^{15}N$-gly]GSH and a NADPH regenerating system. The product ion nominal mass spectrum (E) was included to show the presence of the diagnostic product ion at $m/z$ 286, which was not detected by Orbitrap due to its low abundance.

marked differences in the relative abundances of $m/z$ 676 and 387 compared to the conjugate from the addition of glutathione to the $\beta$-carbon atom. Therefore, GSM1 and GSM2 were tentatively assigned the isomeric structures of glutathion-*S*-yl-dihydroxy-pyrrolidinyl-**1** as illustrated in Figures 10 and 11, respectively. The chemical formula of $[M + H]^+$, together with the product ions at nominal $m/z$ 601, 547, 401, 403, and 369 of GSM3, permitted tentative assignment of glutathion-*S*-yl-pyrrolidinone-**1** as a potential structure for GSM3. These product ions were from identical bond cleavages that resulted in the corresponding product ions at $m/z$ 619, 565, 419, 421, and 387 from either GSM1 or GSM2.

Isomers of glutathion-*S*-yl-dihydroxy-pyrrolidinyl-**1** (GSM1 and GSM2) were postulated to derive from an addition of a glutathione molecule to an epoxide reactive intermediate following bioactivation of the hypothetical precursor hydroxy-enamine-**1**. Proof for such a bioactivation pathway may be provided by replacement with hydroxy-enamine-**1** in the trapping experiment. However, this metabolite was not detected in liver S9 incubates, and proof for this pathway was investigated instead with the speculated penultimate precursor enamine-**1** (Supporting Information). Incubation of ~0.05 $\mu$M of enamine-**1**, under similar conditions used for trapping GSH conjugates, led to the detection of 2 peaks with retention times close to those of GSM1 and GSM2 from the incubation of 100 $\mu$M **1** (Supporting Information Figure 2B and C). These two conjugates gave product ion mass spectra that were weak but similar to those of GSM1 and GSM2 (data not shown). Furthermore, these conjugates were absent from a similar incubation of enamine-**1** where NADPH was omitted (Supporting Information Figure 2A). In addition, a small peak was also detected following the incubation of enamine-**1** with a retention time close to that of glutathion-*S*-yl-pyrrolidinone-1 (GSM3) from the incubation of 100 $\mu$M **1** (Supporting Information Figure 2E and F). The CID of the $[M + H]^+$ of this small peak gave a base peak identical to that of GSM3 at $m/z$ 547 from the loss of pyroglutamic acid (data not shown). Hence, these glutathione conjugates (GSM1−3) were also detected from the replacement of **1** with enamine-**1** in similar incubations used for trapping GSH conjugates. This provided evidence for the presence of the enamine functionality in the precursors of these glutathione conjugates and allowed


dx.doi.org/10.1021/tx1004437 |*Chem. Res. Toxicol.* 2011, 24, 1012–1030

tentative assignment of their structures. However, other potential structures for these GSH conjugates cannot be totally excluded in the absence of definitive NMR data.

## DISCUSSIONS

During early development, **1** was identified as a mutagen in strain TA1537 in the GLP 5-strain Ames test and in the Mouse Lymphoma L5178Y assay. Both assays gave positive readouts only when supplemented with Aroclor 1254-induced rat liver S9 and the NADPH-regenerating system. The need for metabolic activation for the mutagenic responses of **1** in both *in vitro* genotoxicity assays clearly pointed to the involvement of metabolic product(s) in its mutagenicity (Figure 2). Metabolites of **1** were postulated to cause mutagenicity via either simple intercalation due to the planar structure of the arylindenopyrimidine scaffold or from covalent adduction. It has been reported that there is a good correlation between covalent DNA binding and *in vitro* genotoxicity assays including the Ames test.[20]

Therefore, the mechanism of mutagenicity was investigated using surrogate readouts from the covalent binding of [$^3$H]-**1** to DNA in the presence and absence of a metabolic activation system. Metabolic activation resulted in greater nonextractable radioactivity bound to calf thymus DNA. This suggested a high probability of covalent binding of the reactive metabolite to DNA (Table 1). The direct incubation with DNA led to low amounts of nonextractable radioactivity above the background, which suggested a minimum contribution of simple intercalation between DNA base-pairs to the mutagenicity of **1**. This is because the mechanism of frame-shift mutations in strain TA1537 has been associated with simple intercalators.[10,11] Instead, the covalent binding to DNA with metabolic activation together with about 46% and 58% reduction in this event by methoxylamine and cyanide ion, respectively, supported a mechanism involving covalent adduction of DNA by aldehyde and iminium ion reactive intermediates. However, the near complete protection of covalent binding of **1** to DNA in the presence of both methoxylamine and cyanide ion pointed to the involvement of both reactive intermediates in the genotoxicity of **1**. There was minimum, if any, involvement of soft electrophiles in the mutagenicity of **1** on the basis of negligible protective effect by glutathione. Overall, the data supported the covalent adduction of reactive metabolites to DNA as the predominant mechanism for the frame-shift mutation of **1** in tester strain TA1537. This conclusion was consistent with previous findings where covalent adduction played a greater role than simple intercalation in total mutagenic expression of acridine[11] and its analogues[12] in bacterial tester strains including TA1537. This metabolic activation-dependent covalent binding to DNA was also observed with human liver S9 but with about 3-fold less covalent binding to DNA. This approximately 3-fold less covalent binding to DNA by human liver S9 was obtained despite the formation of comparable amounts of cyano conjugates as those in rat S9. It was speculated that species differences in further disposition of the iminium ion reactive intermediates may be responsible for the difference in covalent DNA binding. Therefore, this covalent DNA binding data provided relevance for extrapolation of the *in vitro* genotoxicity data in rodents to human. This is helpful especially in the absence of data from Ames tests conducted with human liver S9.

Elucidation of reactive intermediate structures from both enzymatic and chemical hydrolysis of covalently modified DNA to modified deoxyribonucleosides and nucleobases was not successful. Therefore, an indirect approach was taken for elucidation of the reactive metabolite responsible for genotoxicity of **1** since **1** has multiple structural alerts for potentially forming reactive metabolites (Figure 1). Furthermore, it was demonstrated that covalent binding of [$^3$H]-**1** to DNA could be reduced by competing for binding to reactive metabolites using appropriate chemical trapping agents such as cyanide ion and methoxylamine. From these incubations, 2-cyano-5-pyrrolidinone-**1** (CNM1) and 2,5-dicyanopyrrolidinyl-**1** (CNM2 and CNM3) conjugates were detected using similar conditions used to investigate the covalent binding of [$^3$H]-**1** to DNA. The NADPH-dependent formation of these 3 cyano conjugates in Aroclor 1254-induced rat liver S9 was consistent with cytochrome P-450 (CYP450) metabolism-dependent adduct formation. This was corroborated by inhibition of the formation of 2-cyano-5-pyrrolidinone-**1** by a nonspecific CYP450 inhibitor SKF-525A.[21] The effect of SKF-525A on the formation of the 2,5-dicyano conjugates CNM2 and CNM3 was not investigated since they were barely detectable. The product ion mass spectra for all 3 cyano conjugates suggested the addition of cyanide ion to the α-carbon atom of the pyrrolidine ring. Therefore, this supported the bioactivation of **1** to the reactive endocyclic iminium ion intermediates. Interestingly, no 2-cyano-pyrrolidinyl-**1** was detected from the incubation of **1** even at the shortest incubation time of 5 min. Instead, the major cyano conjugate based on radiochemical tagging with [$^{14}$C]-CN was identified as 2-cyano-5-pyrrolidinone-**1** product on the basis of the absence of it forming an oxime derivative and inhibition of its formation by the aldehyde oxidase inhibitor, menadione.[22] The data provided support for rapid metabolism of 2-cyano-pyrrolidinyl-**1** to the reactive 2-cyano endocyclic iminium ion intermediate. This iminium ion intermediate was subsequently metabolized to 2-cyano-5-pyrrolidinone-**1** by aldehyde oxidase since this enzyme has been reported to catalyze the metabolism of iminium ions to lactam metabolites.[22−26]

Alternatively, the 2-cyano endocyclic iminium ion underwent nucleophilic 1,2-addition by another cyanide ion to form the 2,5-dicyanopyrrolidinyl-**1** conjugates CNM2 and CNM3. Unfortunately, no 2-cyano-pyrrolidinyl-**1** was available for further incubation to provide evidence for the formation of the 2,5-dicyanopyrrolidine-**1** conjugate. However, there is precedence for such a biotransformation pathway based on further metabolism of 1-benzyl-2-cyanopyrrolidine to 1-benzyl-2,5-dicyanopyrrolidine.[27] It has been established experimentally that the major 2-cyano-5-pyrrolidinone-**1** conjugate was formed following further metabolism of 2,5-dicyanopyrrolidine-**1** but not from γ-lactam-**1**. These data provide evidence for α-carbon hydroxylation of 2,5-dicyanopyrrolidinyl-**1** to form an aminocyanohydrin moiety, which spontaneously converts to a lactam functionality of 2-cyano-5-pyrrolidinone-**1**. Such a metabolic conversion has also been observed for 1-benzyl-2,5-dicyanopyrrolidine.[27] Hence, the major 2-cyano-5-pyrrolidinone-**1** conjugate could be derived from α-carbon hydroxylation of 2,5-dicyanopyrrolidinyl-**1** and from further metabolism of the 2-cyano endocyclic iminium ion by aldehyde oxidase.

In addition to the cyano conjugates, 2 major and immediate downstream metabolites consistent with the bioactivation of **1** to endocyclic iminium ions were also detected from the incubation of **1**. These metabolites included the second most abundant γ-lactam-**1** ([peak area of γ-lactam-**1**/peak area of **1**] × 100: ∼6%), which was postulated to derive from further metabolism

of the endocyclic iminium ion of **1** by aldehyde oxidase. This is corroborated by an approximate 3- and 4-fold greater formation of γ-lactam-**1** and 2-cyano-5-pyrrolidinone-**1** by rat liver S9 compared to microsomes. The major endocyclic enamine-**1** ([peak area of enamine-**1**/peak area of **1**] × 100: ∼18%) was speculated to derive from reversible acid-based catalyzed isomerization of endocyclic iminium ion or from dehydration of the endocyclic α-carbinolamine-**1** as previously observed for alicyclic amines.[24,26,28,29] These cyano conjugates together with the detected γ-lactam-**1** and endocyclic enamine-**1** provided evidence for the bioactivation of **1** to the reactive endocyclic iminium ion intermediate by Aroclor 1254-induced rat liver S9. This bioactivation of **1** to reactive endocyclic iminium ion intermediates was also observed in human liver S9 as indicated by the detection of all 3 cyano conjugates. The metabolic formation of 2-cyano-5-pyrrolidinone-**1** from 2,5-dicyanopyrrolidinyl-**1** provided indirect evidence for α-carbon hydroxylation of the pyrrolidine ring. This CYP450-mediated α-carbon hydroxylation of the pyrrolidine ring was proposed as a potential pathway to the formation of the endocyclic iminium ion intermediate via hydrolytic equilibrium with the endocyclic α-carbinolamine-**1** intermediate.[23,30] This endocyclic α-carbinolamine-**1** was unstable because no metabolite from hydroxylation of the pyrrolidine ring was detected from the incubation of **1**. Alternatively, the formation of the endocyclic iminium ion is speculated to involve a direct CYP450-mediated 2-electron oxidation of the pyrrolidine ring based on the mechanism of formation of the nicotine $\Delta^{1'(5')}$ iminium ion.[24] It was further speculated that another CYP450-mediated oxidation of 2-cyano-pyrrolidinyl-1 led to the formation of the 2-cyano endocyclic iminium ion. This was followed by 1,2-addition by another cyanide ion to form the 2,5-dicyano conjugate.

Reactive aldehyde metabolite intermediates were trapped as oxime conjugates. The reversible decomposition of the endocyclic α-carbinolamine-**1** to a ring-opened amino aldehyde-**1** intermediate was trapped as a pair of oxime conjugates OM3 and OM4. This metabolic processing of endocyclic α-carbinolamine-**1** is frequently observed from the metabolism of cyclic tertiary amines.[24−26,31] Also detected was a ring-closed oxime conjugate of a monounsaturated ring-opened amino aldehyde-**1** (OM5). This is based on the reported oxime conjugate of an antiobesity compound to exist in both ring-opened and ring-closed forms.[4] The site of unsaturation could be either α,β or β,γ to the aldehyde functionality but could not be established by tandem mass spectrometry. The formation of aldehyde-**1** metabolite intermediate, inferred from the pair of oxime conjugates OM1 and OM2, was speculated to derive from N-dealkylation of the exocyclic α-carbinolamine-**1** formed in equilibrium with an exocyclic iminium ion.[24,26,28] Attempts to detect the complementary pyrrolidine metabolite from the incubation of **1** were not successful. This may be due to low mass spectrometric response from ion suppression by coeluting polar compounds because of its elution slightly after the void volume of the column. This N-dealkylation reaction has been reported to proceed faster than the addition of cyanide ion,[28] which explained the failure to trap the exocyclic iminium ion of **1**. The data generated provided evidence for the bioactivation of **1** to ring-opened amino aldehyde-**1** metabolite intermediate from decomposition of endocyclic α-carbinolamine-**1** in equilibrium with an endocyclic iminium ion of **1**. Another aldehyde-**1** metabolite intermediate was from the N-dealkylation of an exocyclic α-carbinolamine-**1** intermediate in equilibrium with an exocyclic iminium ion of **1**.

In addition to detecting the cyano- and oxime-conjugates, GSH conjugates were also detected (GSM1−3). A pair of regioisomeric glutathion-*S*-yl-dihydroxy-pyrrolidinyl-**1** (GSM1 and GSM2) conjugates was postulated from the addition of a GSH molecule to an epoxide reactive intermediate. The epoxide was localized to the pyrrolidine ring of **1** by CID of the GSH conjugates GSM1 and GSM2. The formation of both GSH conjugates was speculated to derive from bioactivation of a postulated hydroxy-enamine-**1**. This is extrapolated from the reported bioactivation of an enamine metabolite of a piperidine-containing compound to an epoxide reactive intermediate.[26,28] The detection of both conjugates GSM1 and GSM2 from the replacement of enamine-**1** in the trapping experiment corroborated the epoxide as their likely reactive intermediate precursor. The hydroxy group of the postulated precursor, hydroxy-enamine-**1**, could be located at either the α- or the β-position of the pyrrolidine ring of **1**. The failure to detect 2-cyano-enamine-**1** following the incubation of **1** suggested the hydroxy group was likely to be in the β-position. As a result, we hypothesized that the GSH conjugates GSM1 and GSM2 were formed following the bioactivation of 3-hydroxy-enamine-**1**. GSM3 (glutathion-*S*-yl-pyrrolidinone-**1**) was speculated to derive from the addition of a GSH molecule to the α,β-unsaturated keto moiety of the 3-keto-enamine-**1** metabolite. The detection of conjugate GSM3 from the trapping experiment with enamine-**1** suggested the metabolism of enamine-**1** to 3-hydroxy-enamine-**1**, which further oxidized to the putative 3-keto-enamine-**1** metabolite. Precedence for such a metabolic pathway is based on the reported liver microsomal metabolism of phencyclidine iminium ion to the α,β-unsaturated keto product.[32] The data from trapping reactive intermediates together with the identification of immediate stable metabolites supported the postulated *in vitro* bioactivation pathways of **1** as presented in Scheme 1.

Data from reactive intermediate trapping experiments provided evidence for the bioactivation of **1** to the iminium ion, aldehyde, α,β-unsaturated keto and epoxide reactive intermediates by Aroclor 1254-induced rat liver S9. It was unlikely that the latter 2 reactive intermediates trapped by GSH are responsible for the genotoxicity of **1**. This is because GSH did not block the covalent binding of **1** to DNA. Conversely, the endocyclic iminium ion and aldehyde reactive intermediates are likely candidates for causing the genotoxicity of **1**. This is because both endocyclic iminium ion and aldehyde reactive intermediates were implicated in covalent DNA binding based on protection from this event by cyanide ion and methoxylamine, respectively. Furthermore, iminium ion and aldehyde reactive intermediates are intrinsically reactive and have been reported to bind covalently to DNA.[33,34] It was speculated that inhibition of CYP450-mediated bioactivation of **1** to an endocyclic iminium ion intermediate may be effective in the prevention of the genotoxicity of **1** if the mechanism of genotoxicity involved both endocyclic iminium ion and amino aldehyde reactive intermediate formation. This is because the endocyclic iminium ions are frequently formed in equilibrium with endocyclic α-carbinolamine and amino aldehyde reactive intermediates.[26] The covalent bindings of these reactive intermediates of **1** with DNA nucleobase are speculated to proceed via nucleophilic displacement and Schiff base reactions reported for covalent binding of anthramycin with DNA.[34] Furthermore, the electrophilic amino aldehyde and iminium ion reactive intermediates were proposed to be responsible for genotoxicity of the antiobesity agent [2-(3-chlorobenzyloxy)-6-(piperazin-1-yl)pyrazine,[7] which provided

**Scheme 1. Proposed *in Vitro* Bioactivation Pathways of 1 by Aroclor 1254-Induced Rat Liver S9**[a]

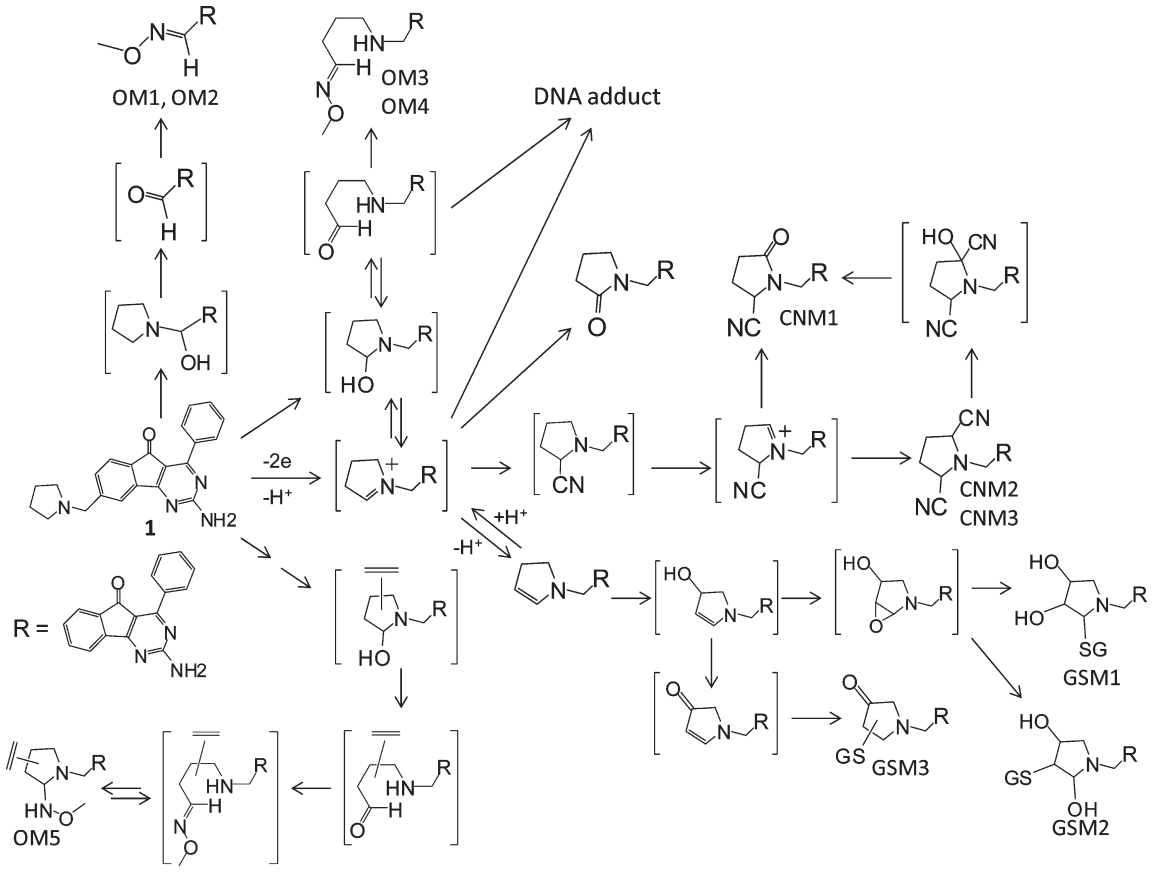


[a] The pathway denoted by 2 arrows involved multiple metabolic steps. Structures in brackets were not detected by LC-MS.

precedence for our current hypothesis. The translation of this hypothesis of the genotoxicity mechanism for **1** led to the synthesis of 2 structural analogues for proof-of-concept follow up studies in the Ames assay. Analogue **2** was synthesized with reduced potential for genotoxicity based on a strategy of decreasing the formation of endocyclic iminium ion and amino aldehyde reactive intermediates by steric hindrance via the methylation of both pyrrolidinyl α-carbons. Another analogue, **3**, was synthesized with no potential for bioactivation to both reactive intermediates by replacing the pyrrolidine moiety with a pyridine ring. Furthermore, **3** was also designed to check for bioactivation of the 8-methyl-arylindenopyrimidine moiety of **1**. Evaluation of both **2** and **3** in a reverse mutation Ames test gave negative genotoxicity for all 5 strains tested including TA1537. Negative genotoxicity with both **2** and **3** supported the genotoxicity of **1** was caused by bioactivation to endocyclic iminium ion and amino aldehyde reactive intermediates. This was consistent with no detection of the endocyclic iminium ion from coincubation of **2** with the cyanide ion. This approach of designing out genotoxicity liability was achieved by minimizing the formation of iminium ions via methyl substitution of both α-carbons of the pyrrolidine ring of **1**. Such an approach in reducing iminium ion formation was successfully applied to overcome the genotoxicity of [2-(3-chlorobenzyloxy)-6-(piperazin-1-yl)pyrazine[35] and decreased high covalent protein binding of a piperazine-containing compound.[36] The negative result with **3** confirmed that the reactive aldehyde-**1** intermediate, from N-dealkylation of exocyclic α-carbinolamine-**1**, was not involved in the genotoxicity of **1**. Furthermore, it was unlikely that there was bioactivation of the arylindenopyrimidine scaffold to form arene oxide or nitroso reactive intermediates. Most importantly, these 2 analogues retained pharmacological activity with comparable potency and selectivity against the $A_{2A}$ and $A_1$ receptors.

The absence of genotoxicity for analogues **2** and **3** provide persuasive evidence that pyrrolidine ring bioactivation to endocyclic iminium ion and amino aldehyde reactive intermediate products were pivotal, aberrant, metabolic events for **1**. The arylindenopyrimidine moiety was a viable scaffold for the synthesis of dual $A_{2A}/A_1$ adenosine receptor antagonists and did not represent a genotoxicity liability. This case study clearly illustrates that pursuing a mechanistic understanding of the metabolism-mediated genotoxicity of **1** led to a focused medicinal chemistry effort to generate analogues **2** and **3** for timely introduction of a product into the drug development pipeline with a markedly improved safety profile.

## ■ ASSOCIATED CONTENT

**Supporting Information.** Characterization of γ-lactam-**1** and enamine-**1**, *in vitro* metabolism of both isomers of 2,5-dicyanopyrrolidinyl-**1** to 2-cyano-5-pyrrolidinone-**1**, and trapping of glutathion-*S*-yl-dihydroxy-pyrrolidinyl-1 (GSM1 and GSM2) and glutathion-*S*-yl-pyrrolidinone-**1** (GSM3) from *in vitro* metabolism of enamine-**1** as mentioned in the text.

This material is available free of charge via the Internet at http://pubs.acs.org.

## AUTHOR INFORMATION

### Corresponding Author

*Drug Metabolism and Pharmacokinetics, Drug Safety Sciences, Johnson and Johnson Pharmaceutical Research and Development, 1000 Route 202 South, NJ 08869. E-mail: hlim5@its.jnj.com.

## ACKNOWLEDGMENT

We acknowledge Alfred Barron and Dhammika Amaratunga for statistical analysis of data from the Ames test, Tony Greway and Mark Johnson for sharing and discussing DMPK and toxicology data, and Shannon Dallas and Monica Singer for help with spectrophotometric quantitation of DNA.

## ABBREVIATIONS

PD, Parkinson's disease; DA, dopamine; DOPA, L-dihydroxyphenylalanine; NADPH, reduced nicotinamide adenine dinucleotide phosphate; GSH, glutathione; KCN, potassium cyanide; LC-RAD-MS, liquid chromatography−radioactivity detector−mass spectrometry; LC-MS, liquid chromatography−mass spectrometry; H/D, hydrogen/deuterium; $D_2O$, deuterium oxide; RDB, rings plus double-bonds; $[M + H]^+$, protonated molecule; CID, collision-induced dissociation; RIC, reconstructed ion chromatogram; RRT, retention time relative to unchanged drug; **1**, 2-amino-4-phenyl-8-pyrrolidin-1-ylmethyl-indeno[1,2-d]-pyrimidin-5-one; **2**, 2-amino-8-(2,5-dimethyl-pyrrolidin-1-yl-methyl)-4-phenyl-indeno[1,2-d]pyrimidin-5-one; **3**, 2-amino-4-phenyl-8-pyridin-3-ylmethyl-indeno[1,2-d]pyrimidin-5-one.

## REFERENCES

(1) Goetz, C. G. (1992) Parkinson's Disease and Other Parkinsonian Syndromes, in *Textbook of Clinical Neuropharmacology and Therapeutics* (Klawans, H. L., Goetz, C. G., and Tanner, C. M., Eds.) pp 91−116, Raven Press, New York.

(2) Shook, B. C., Rassnick, S., Hall, D., Rupert, K. C., Heintzelman, G. R., Hansen, K., Chakravarty, D., Bullington, J. L., Scannevin, R. H., Magliaro, B., Westover, L., Carroll, K., Lampron, L., Russell, R., Branum, S., Wells, K., Damon, S., Youells, S., Li, Y., Osbourne, M., Demarest, K., Tang, Y. T., Rhodes, K., and Jackson, P. (2010) Methylene amine substituted arylindenopyrimidines as potent adenosine $A_{2A}/A_1$ antagonist. *Bioorg. Med. Chem. Lett. 20*, 2864–2867.

(3) Maron, D. M., and Ames, B. N. (1984) Revised methods for the *Salmonella* mutagenicity test. *Mutat. Res. 113*, 173–215.

(4) Kalgutkar, A. S., Dalvie, D. K., Aubrecht, J., Smith, E. B., Coffing, S. L., Cheung, J. R., Vage, C., lame, M. E., Chiang, P., McClure, K. F., Maurer, T. S., Coelho, R. V., Soliman, V. F., and Schildknegt, K. (2007) Genotoxicity of 2-(3-chlorobenzyloxy)-6-(piperazinyl)pyrazine, a novel 5-hydroxytryptamine$_{2c}$ receptor agonist for the treatment of obesity: Role of metabolic activation. *Drug Metab. Dispos. 35* (6), 848–858.

(5) Zhang, S. Y., Villalta, P. W., Wang, M. Y., and Hecht, S. S. (2006) Analysis of crotonaldehyde- and acetaldehyde-derived 1,$N^2$-propanodeoxyguanosine adducts in DNA from human tissues using liquid chromatography-electrospray ionization-tandem mass spectrometry. *Chem. Res. Toxicol. 19* (10), 1386–1392.

(6) Rindgren, D., Nakajima, M., Wehrli, S., Xu, K. Y., and Blair, I. A. (1999) Covalent modifications to 2′-deoxyguanosine by 4-oxo-2-nonenal, a novel product of lipid peroxidation. *Chem. Res. Toxicol. 12*, 1195–1204.

(7) Lim, H. K., Chen, J., Cook, K., Sensenhauser, C., Silva, J., and Evans, D. C. (2008) A generic method to detect electrophilic intermediates using isotopic pattern triggered data-dependent high-resolution accurate mass spectrometry. *Rapid Commun. Mass Spectrom. 22* (8), 1295–1311.

(8) Nasser, A. E., and Lee, D. Y. (2007) Novel approach to performing metabolite identification in drug metabolism. *J. Chromatogr. Sci. 45* (3), 113–119.

(9) Knapp, D. R. (1979) *Handbook of Analytical Derivatization Reactions*, pp 151−224 and 338−386, Wiley, New York.

(10) Ames, B. N., Lee, F. D., and Durston, W. F. (1973) An improved bacterial test system for the detection and classification of mutagens and carcinogens. *Proc. Natl. Acad. Sci. U.S.A. 70*, 782–786.

(11) Brown, B. R., Firth, W. J., III, and Yielding, L. W. (1980) Acridine structure correlated with mutagenic activities in *Salmonella*. *Mutat. Res. 71*, 373–388.

(12) McCoy, E. C., Rosenkranz, E. J., Petrullo, L. A., Rosenkranz, H. S., and Mermelstein, R. (1981) Frameshift mutations: Relative roles of simple intercalation and of adduct formation. *Mutat. Res. 90* (1), 21–30.

(13) Salter, R. (2010) The development and use of iridium (I) phosphine systems for ortho-directed hydrogen-isotope exchange *J. Labelled Comp. Radiopharm. 53* (11−12), 645–657.

(14) Santella, R. M., Grunberger, D., and Weinstein, I. B. (1979) DNA-benzo[*a*]pyrene adducts formed in a *Salmonella typhimurium* mutagenesis assay system. *Mutat. Res. 61*, 181–189.

(15) Shigenaga, M. K., Trevor, A. J., and Castagnoli, N., Jr. (1988) Metabolism-dependent covalent binding of (*S*)-[5-$^3$H]nicotine to liver and lung microsomal macromolecules. *Drug Metab. Dispos. 16* (3), 397–402.

(16) Kitada, M., Chiba, K., Kamataki, T., and Kitagawa, H. (1977) Inhibition by cyanide of drug oxidations in rat liver microsomes. *Jpn. J. Pharmacol. 27*, 601–608.

(17) Zhang, C. H., Wong, S., Delarosa, E. M., Kenny, J. R., Halladay, J. S., Hop, C. E., and Khojasteh-Bakht, S. C. (2009) Inhibitory properties of trapping agents: glutathione, potassium cyanide, and methoxylamine against major human cytochrome P450 isoforms. *Drug Metab. Lett. 3*, 125–129.

(18) Argoti, D., Liang, L., Conteh, A., Chen, L. F., Bershas, D., Yu, C. P., Vouros, P., and Yang, E. (2005) Cyanide trapping of iminium ion reactive intermediates followed by detection and structure identification using liquid chromatography-tandem mass spectrometry (LC-MS/MS). *Chem. Res. Toxicol. 18* (10), 1537–1544.

(19) Haroldsen, P. E., Reilly, M. H., Hughes, H., Gaskell, S. J., and Porter, C. J. (1988) Characterization of glutathione conjugates by fast atom bombardment/tandem mass spectrometry. *Biomed. Environ. Mass Spectrom. 15*, 615–621.

(20) Taningher, M., Saccomanno, G., Santi, L., Grilli, S., and Parodi, S. (1990) Quantitative predictability of carcinogenicity of the covalent binding index of chemicals to DNA: Comparison of the *in vivo* and *in vitro* assays. *Environ. Health Perspect. 84*, 183–192.

(21) Franklin, M. R., and Hathaway, L. B. (2008) 2-Diethylaminoethyl-2,2-diphenylvalerate-HCl (SKF525A) revisited: comparative cytochrome P450 inhibition in human liver microsomes by SKF525A, its metabolites, and SKF-acid and SKF-alcohol. *Drug Metab. Dispos. 36* (12), 2539–2546.

(22) Rajagopalan, K. V., and Handler, P. (1964) Hepatic aldehyde oxidase. II. Differentiation inhibition of electron transfer to various electron acceptors. *J. Biol. Chem. 239*, 2022–2026.

(23) Gorrod, J. W., and Aislaitner, G. (1994) The metabolism of alicyclic amines to reactive iminium ion intermediates. *Eur. J. Drug Metab. Pharmacokinet. 19* (3), 209–217.

(24) Murphy, P. J. (1973) Enzymatic oxidation of nicotine to nicotine $\Delta^{1'(5')}$ iminium ion. *J. Biol. Chem. 248* (8), 2796–2800.

(25) Brandange, S., Lindblom, L., Pilotti, A., and Rodriguez, B. (1983) Ring-chain tautomerism of pseudooxynicotine and some other iminium compounds. *Acta Chem. Scand. B 37*, 617–622.

(26) Sayre, L. M., Engelhart, D. A., Nadkarni, D. V., Manoj Babu, M. K., Flammang, A. M., and McCoy, G. D. (1997) The Role of Iminium-Enamine Species in the Toxication and Detoxification of Cyclic Tertiary Amines, in *Pharmacokinetics, Metabolism and Pharmaceutics of Drugs of*

*Abuse* (Rapaka, R. S., Chiang, N., and Martin, B. R., Eds.) pp 106−127, National Institute on Drug Abuse Research Monograph 173, DHHS Pub. No. (ADM) 91−1754, Supt. of Docs., U.S. Govt. Print. Off., Washington, DC.

(27) Ho, B., and Castagnoli, N., Jr. (1979) Trapping of metabolically generated electrophilic species with cyanide ion: Metabolism of 1-benzylpyrrolidine. *J. Med. Chem. 23*, 133–139.

(28) Masumoto, H., Ohta, S., and Hirobe, M. (1991) Application of chemical cytochrome P-450 model systems to studies on drug metabolism. IV. Mechanism of piperidine metabolism pathways via an iminium intermediate. *Drug Metab. Dispos. 19* (6), 768–780.

(29) Burrows, W. D., and Burrows, E. P. (1963) $\beta$-Condensation reactions of cyclic amines with benzaldehyde: evidence for the enamine pathway. *J. Org. Chem. 28*, 1180–1182.

(30) Petersen, L. A., and Castagnoli, N., Jr. (1988) Regio- and stereochemical studies on the $\alpha$-carbon oxidation of (S)-nicotine by cytochrome P-450 model systems. *J. Med. Chem. 31*, 637–640.

(31) Nguyen, T. L., Dagne, E., Gruenke, L., Bhargava, H., and Castagnoli, N., Jr. (1981) The tautomeric structures of 5-hydroxynicotine, a secondary mammalian metabolite of nicotine. *J. Org. Chem. 46*, 758–760.

(32) Hoag, M. K. P., Schmidt-Peetz, M., Lampen, P., Trevor, A., and Castagnoli, N., Jr. (1988) Metabolic studies on phencyclidine: Characterization of a phencyclidine iminium ion metabolite. *Chem. Res. Toxicol. 1*, 128–131.

(33) Moore, B. M., Seaman, F. C., Wheelhouse, R. T., and Hurley, L. (1998) Mechanism for the catalytic activation of ecteinascidin 743 and its subsequent alkylation of guanine N2. *J. Am. Chem. Soc. 120*, 2490–2491.

(34) Hurley, L. H., and Thurston, D. E. (1984) Pyrrolo-(1,4)benzodiazepine antitumor antibiotics: Chemistry, interaction with DNA, and biological implications. *Pharm. Res. 1* (2), 52–59.

(35) Kalgutkar, A. S., Fate, G., Didiuk, M. T., and Bauman, J. (2008) Toxicophores, reactive metabolites and drug safety: when is it a cause for concern? *Expert Rev. Clin. Pharmacol. 1* (4), 515–531.

(36) Kumar, S., Kassahun, K., Tschirret-Guth, R. A., Mitra, K., and Baillie, T. A. (2008) Minimizing metabolic activation during pharmaceutical lead optimization: Progress, knowledge gaps and future directions. *Curr. Opin. Drug Discovery Dev. 11*, 43–52.